



ECOLOGY

Resistance to freezing conditions of endemic Antarctic polychaetes is enhanced by cryoprotective proteins produced by their microbiome

Emanuela Buschi^{1,2}, Antonio Dell'Anno², Michael Tangherlini³, Marco Candela^{4,5}, Simone Rampelli^{4,5}, Silvia Turrone⁴, Giorgia Palladino^{4,5}, Erika Esposito^{6,7}, Marco Lo Martire², Luigi Musco⁸, Sergio Stefanni⁹, Cristina Munari¹⁰, Jessica Fiori^{6,7}, Roberto Danovaro², Cinzia Corinaldesi^{11*}

Copyright © 2024 the Authors, some rights reserved; exclusive licensee American Association for the Advancement of Science. No claim to original U.S. Government Works. Distributed under a Creative Commons Attribution NonCommercial License 4.0 (CC BY-NC).

The microbiome plays a key role in the health of all metazoans. Whether and how the microbiome favors the adaptation processes of organisms to extreme conditions, such as those of Antarctica, which are incompatible with most metazoans, is still unknown. We investigated the microbiome of three endemic and widespread species of Antarctic polychaetes: *Leitoscoloplos geminus*, *Aphelochaeta palmeri*, and *Aglaophamus trissophyllus*. We report here that these invertebrates contain a stable bacterial core dominated by *Meiothermus* and *Anoxybacillus*, equipped with a versatile genetic makeup and a unique portfolio of proteins useful for coping with extremely cold conditions as revealed by pangenomic and metaproteomic analyses. The close phyllosymbiosis between *Meiothermus* and *Anoxybacillus* and these Antarctic polychaetes indicates a connection with their hosts that started in the past to support holobiont adaptation to the Antarctic Ocean. The wide suite of bacterial cryoprotective proteins found in Antarctic polychaetes may be useful for the development of nature-based biotechnological applications.

INTRODUCTION

Multicellular organisms in the oceans live in close association with their microbiomes, which provide their hosts with key functions including nutrient supply, defense mechanisms, and even additional metabolic pathways, thus representing an integral component of the holobiont, able to influence host physiology and increase adaptation to environmental conditions (1–3). Microbiome-host interactions are far more widespread than previously thought and can notably influence the auto-ecology of marine organisms, playing a role in the whole ecosystem's health (4–6).

The host-associated microbiota changes from species to species, also in relation to a variety of environmental (i.e., geographic location, seasonal variations, and nutrient availability) (7, 8) and biological factors (i.e., metabolic state, feeding strategy, and host phylogeny) (9, 10). However, the presence of a stable core (i.e., any set of microbial taxa characteristic of a specific host or environment) (11), reported for several holobionts, suggests that some microbes and related genomic or functional features are essential for the well-being of the host species (12, 13).

Some specific bacterial taxa, indeed, can be vertically transmitted and persist across life stages and generations, favoring mutual adaptation (2, 14). Mechanisms of transmission of microbiome components to their hosts may include horizontal acquisition, which is generally based on a selection of beneficial bacterial members from the environment anew by each host generation (15, 16).

Microbiomes could also have a role in the host-microbe adaptation to extreme environmental conditions and in evolutionary processes (2, 17). In this regard, information on marine host-microbiota phyllosymbiosis as an eco-evolutionary pattern, where the ecological relatedness of host-associated microbial communities parallels the phylogeny of related host species (18), is contrasting. In some organisms, phyllosymbiosis has been documented even to different extents in specific portions of their body (2, 19), whereas in others, it seems not to have a primary role, suggesting the lack of strong affinity between bacterial members and their specific host lineage (20).

The processes driving microbial associations and influencing the adaptations of marine organisms to environmental conditions are still open questions (21). The investigation in extreme ecosystems can certainly contribute to explore the co-evolutionary processes and ecological interactions of the microbiota-host associations. One of the most isolated continents on Earth, Antarctica, can provide additional information into the adaptation of marine life to extreme conditions.

The geological isolation, along with the stability of extreme environmental conditions, for more than 34 million years has produced a range of unique adaptations to low temperatures with a highly diverse fauna composed of around 17,000 marine invertebrate species and with the highest proportions of endemic species of the world ocean (22, 23).

In polar ecosystems, marine poikilotherm metazoans (i.e., in which the internal temperature is in equilibrium with the environmental temperature) must adapt to extreme cold conditions using different biological and physiological mechanisms, such as the slowdown in embryonic development and growth rate and increase in

¹Department of Ecosustainable Marine Biotechnology, Stazione Zoologica "Anton Dohrn," Fano Marine Centre, Fano, Italy. ²Department of Life and Environmental Sciences, Polytechnic University of Marche, Ancona, Italy. ³Department of Research Infrastructures for Marine Biological Resources, Stazione Zoologica "Anton Dohrn," Fano Marine Centre, Fano, Italy. ⁴Department of Pharmacy and Biotechnology, University of Bologna, Bologna, Italy. ⁵Fano Marine Center, the Inter-Institute Center for Research on Marine Biodiversity, Resources and Biotechnologies, Fano, Italy. ⁶Department of Chemistry "G. Ciamician" Alma Mater Studiorum, University of Bologna, Bologna, Italy. ⁷IRCCS Istituto delle Scienze Neurologiche di Bologna, Bologna, Italia. ⁸Department of Biological and Environmental Sciences and Technologies, University of Salento, Lecce, Italy. ⁹Department of Biology and Evolution of Marine Organisms, Stazione Zoologica "Anton Dohrn," Villa Comunale, Napoli, Italy. ¹⁰Department of Chemical and Pharmaceutical Sciences, University of Ferrara, Ferrara, Italy. ¹¹Department of Materials, Environmental Sciences and Urban Planning, Polytechnic University of Marche, Ancona, Italy.

*Corresponding author. Email: c.corinaldesi@univpm.it

oxygen consumption to maintain homeostasis, to prevent internal liquid freezing and to induce the antioxidant defense system (23).

Previous studies also hypothesized the presence of thermal hysteresis proteins in the haemolymph of ectothermic invertebrates, such as Antarctic nemerteans (24) and terrestrial invertebrates (25), but no general conclusions could be provided. At the same time, microbes own functional traits for adaptation to low temperatures (26, 27) and, when associated with Antarctic benthic invertebrates, play key roles in several metabolic processes (28). However, information on the mechanisms adopted by marine invertebrates to cope with extreme cold and freezing conditions is limited and controversial (23, 29), and the role of their microbiota in these mechanisms is even neglected.

In the present study, we investigated the microbiome of three dominant endemic species of Antarctic polychaetes (*Leitoscoloplos geminus*, *Aphelochaeta palmeri*, and *Aglaophamus trissophyllus*; Fig. 1) that play a key role in the benthic trophic webs (30, 31). The identity, origin, and proteome of the microbiota associated with these Antarctic invertebrates, as well as the factors influencing its structure, including phyllosymbiosis, were investigated to provide insights into the role of the microbiome in marine invertebrate adaptation to the extreme conditions of Antarctic ecosystems.

RESULTS

Environmental setting of the study area

The environmental characteristics (temperature, salinity, sediment grain size, and biochemical composition of organic matter) of the three different sampling areas (Adelie Cove, Rod Bay, and Central Bay) of the Ross Sea are reported in table S1 and figs. S2 and S3.

The temperature of the investigated area ranged from -0.29° to -1.09°C at 25-m depth (in Rod Bay and Adelie Cove, respectively), from -1.23° to -1.85°C at 70 m (in Adelie Cove and Central Bay, respectively), and from -1.89° to -1.95°C at 140 m (in Adelie Cove and Central Bay, respectively). Salinity ranged from 33.74 to 34.52 at 25 m (in Rod Bay and Adelie Cove, respectively) and remained stable at around 34.69 at both 70- and 140-m depth in each area, except for Adelie Cove at 70 m where it decreased to 34.32 (table S1).

The grain size analysis revealed significant differences among the sediments of the three sampling areas ($P < 0.001$; table S3), although the fine sand fraction largely contributed to the total sedimentary composition (from 66.3 to 96.6%) in all areas, except for the stations at 25- and 140-m depth of Rod Bay where more than 50% of the grain size was coarser (table S3 and fig. S2).

The amount of food potentially available to benthic consumers (in terms of the biochemical composition of organic matter: lipid, protein, and carbohydrate concentrations) did not show any significant change in the investigated areas (table S3). However, significant differences were found along bathymetric gradients within each area. In Rod Bay, the highest concentrations of phaeopigments, carbohydrates, and lipids were found at 140-m depths ($P < 0.05$; table S3) as well as in Central Bay for the concentrations of phaeopigments and lipids ($P < 0.05$; table S3). In the sediments of Adelie Cove, the highest values of proteins, carbohydrates, lipids, and phaeopigments were found at 70-m depth ($P < 0.01$; table S3 and fig. S3).

Only for the concentrations of chlorophyll-a, a different pattern was observed compared to the other biochemical components (i.e., significant differences were observed between the Central Bay and Adelie Cove areas and among the different depths of Rod Bay) (overall $P < 0.05$; table S3 and fig. S3).

Molecular and phylogenetic analyses of the Antarctic polychaetes

The taxonomic identification of the three species of Antarctic polychaetes was initially carried out by using a classical approach (dichotomous keys under light microscope) and was confirmed by sequencing of mitochondrial genes. For the mitochondrial *16S*, *12S*, and *COI* (cytochrome C oxidase subunit I) genes, high-quality DNA sequences were obtained for both *A. palmeri* and *A. trissophyllus*. Although the primer sets used successfully amplified the *16S* and *12S* fragments of all *L. geminus* specimens, no *COI* sequence was obtained for this polychaete species.

The *16S* sequence alignment and the resulting phylogenetic tree revealed that all 12 sequences of *L. geminus* belonged to the same haplotype. The six sequences of *A. trissophyllus* clustered with those of *Aglaophamus* cf. *trissophyllus* (KX867140.1) and were represented by two shared and two unique haplotypes, with a variability below five nucleotide mutations (table S6 and fig. S4). The 12 sequences of *A. palmeri* were identical and constituted a shared haplotype, which clustered with a sequence of the same genus, *Aphelochaeta marioni* (DQ779602.1). Alignment of the *12S* sequences and the resulting phylogenetic tree revealed that all the 12 sequences of *L. geminus* were identical and that the 9 sequences of *A. trissophyllus* grouped into three shared and three unique haplotypes, with a total of 11 nucleotide variations. The two sequences of *12S* from *A. palmeri* grouped into one shared haplotype (table S6 and fig. S4). Last, the alignment of *COI* sequences and the resulting phylogenetic tree



Fig. 1. Antarctic polychaetes investigated in the present study. Pictures of polychaetes investigated: *Leitoscoloplos geminus* (A), *Aphelochaeta palmeri* (B), and *Aglaophamus trissophyllus* (C).

revealed that the 10 sequences of *A. trissophyllus* were all unique haplotypes, with a total of 90 nucleotide mutations, and that the 15 sequences from *A. palmeri* clustered in three shared and four unique haplotypes with a total of 18 nucleotide mutations, thus confirming the results of the other markers and also highlighting an intraspecific genetic variation (table S6 and fig. S4).

Composition of the Antarctic polychaete microbiome

Metabarcoding analyses of the bacterial 16S ribosomal RNA (rRNA) genes of the three Antarctic polychaete species yielded 1237 to 49,364 sequences (after denoising and chimera removal). Rarefaction curves of the majority of polychaetes samples plateaued at 1237 reads (fig. S5).

The bacteria associated with the three Antarctic polychaetes investigated in this study mainly belonged to the Deinococci, Bacilli, and Gammaproteobacteria classes, representing on average approximately 70% of the total taxonomic composition of microbiomes, followed by the Campylobacteria and Alpha and Betaproteobacteria classes (on average, 12%; fig. S6).

In the microbiome of *L. geminus*, OTU (operational taxonomic unit) richness ranged from 12 to 64 without significant differences among the samples collected in different areas and at different depths (table S3). High intraspecific microbiome variability was observed among specimens in terms of Shannon, Pielou's, and phylogenetic diversity but without significant differences among different areas and depths (fig. S7 and table S3). Similarly, no significant differences were found in microbiome composition among specimens collected in different areas and at different depths (table S3).

Similarity Percentage (SIMPER) analysis, indeed, revealed a 47.8% similarity in microbiome composition among all *L. geminus* specimens (table S4), which shared five bacterial genera (representing, on average, 64% of the total microbiome composition). Among these genera, *Meiothermus* and *Anoxybacillus* contributed to the largest portion (45 and 17%, respectively; Fig. 2). The *Meiothermus* genus was represented by a single OTU assigned to *Meiothermus silvanus*, while the *Anoxybacillus* genus was represented by two OTUs, one of which was affiliated to *Anoxybacillus flavithermus*.

High intraspecific variability was also observed in the OTU richness (from 16 to 44), Shannon and Pielou's indices of the microbiomes of *A. palmeri*. Again, no significant differences were found among the alpha diversity indices of the microbiomes of the specimens collected in different areas and at different depths (fig. S7 and table S3). However, significant differences were found among the microbiome composition of the Adelie Cove and Central Bay samples (table S3). The *A. palmeri* microbiome collected from different areas and depths showed a SIMPER similarity of 43% (table S4), and five bacterial genera were shared among all specimens (accounting, on average, for 64% of the total taxonomic composition): *Meiothermus*, *Anoxybacillus*, *Vulcanibacterium*, *Acinetobacter*, and *Cutibacterium* (mean relative contribution, 11, 30, 12, 9, and 1%, respectively; Fig. 2).

Last, the OTU richness in the microbiome of the different specimens of *A. trissophyllus* ranged from 5 to 34 with no significant differences among the different sampling areas and depths (fig. S7 and table S3). High intraspecific variability was also observed for the other alpha diversity indices. The microbiomes associated with *A. trissophyllus* specimens were characterized by a 32% similarity (table S4). *Meiothermus* was the only genus shared across all specimens, with an average contribution of 42%, and across different body parts within individuals, with an average contribution of 36%

in the gut and parapods, 38% in the oral cavity, and 47% in the tegument (see details in the Supplementary Materials and figs. S9 and S10). *Anoxybacillus* was shared in at least half of the *A. trissophyllus* specimens, with different contributions depending on the polychaete specimen (Fig. 2).

Significant differences in terms of both alpha and beta diversity were found especially between the microbiomes of the predator polychaete *A. trissophyllus* and those of the two detritivorous species, *A. palmeri* and *L. geminus* ($P < 0.05$; figs. S7 and S8 and table S3).

Weighted and unweighted UniFrac distances showed that the microbiomes of detritivorous species (*L. geminus* and *A. palmeri*) clustered apart from the microbiome of predatory species (*A. trissophyllus*) (fig. S8). In particular, the unweighted UniFrac distance resulted in a wider separation.

Meiothermus, *Anoxybacillus*, and *Cutibacterium* were shared among all the specimens of *L. geminus* and *A. palmeri*, and *Meiothermus* was present in all individuals of the three species. Among all the bacterial taxa identified, some were exclusively associated with *L. geminus*, *A. palmeri*, and *A. trissophyllus* (overall contributing 32, 16, and 15% to the total OTU assemblage, respectively). However, these exclusive taxa individually accounted on average for less than 0.5%.

Environmental drivers of the Antarctic polychaete microbiome

The results of the multivariate analysis revealed that the influence of environmental factors on the whole taxonomic composition of microbiomes and the bacterial core was inconsistent or not significant in the different polychaete species (table S5 and fig. S11). However, when excluding bacterial core members of each species (representing, on average, 64% in both *L. geminus* and *A. palmeri* and 42% in *A. trissophyllus*), environmental variables significantly influenced the taxonomic composition of the microbiomes of *A. palmeri*, with the silt-clay concentration being the main driver (64% of total variation; $P < 0.05$; table S5 and fig. S10), and of *L. geminus*, with biopolymeric carbon and chlorophyll-a concentrations explaining 55% of the total variation ($P < 0.05$; table S5 and fig. S11). In contrast, the variability of the taxonomic composition of *A. trissophyllus* microbiomes was not explained by any of the considered factors (table S5 and fig. S11).

The connection between Antarctic polychaete and sediment microbiomes

To assess the origin of the polychaete microbiome, the sediment microbiome was studied in the Antarctic study area. The microbiome in the sediment was characterized by an OTU richness ranging from 167 to 434 (fig. S12). This richness remained rather constant even when several random subsamples of the sequences were carried out. OTU richness and Shannon and Pielou's indices did not significantly change among the three areas, but some significant differences were found among different depths within the areas (table S3 and fig. S12). Similarly, the taxonomic composition of the microbiomes showed no significant differences among the three areas ($P < 0.05$; table S3). Sediment microbiomes showed an average similarity of 60% among samples (table S4). Dissimilarity was mainly due to the different contributions of the *Blastopirellula* genus (from 1.7 to 18.5%) and the Flavobacteriaceae family (from 2.1 to 28.9%).

The microbiomes of polychaetes and sediments were significantly different in terms of alpha and beta diversity and taxonomic

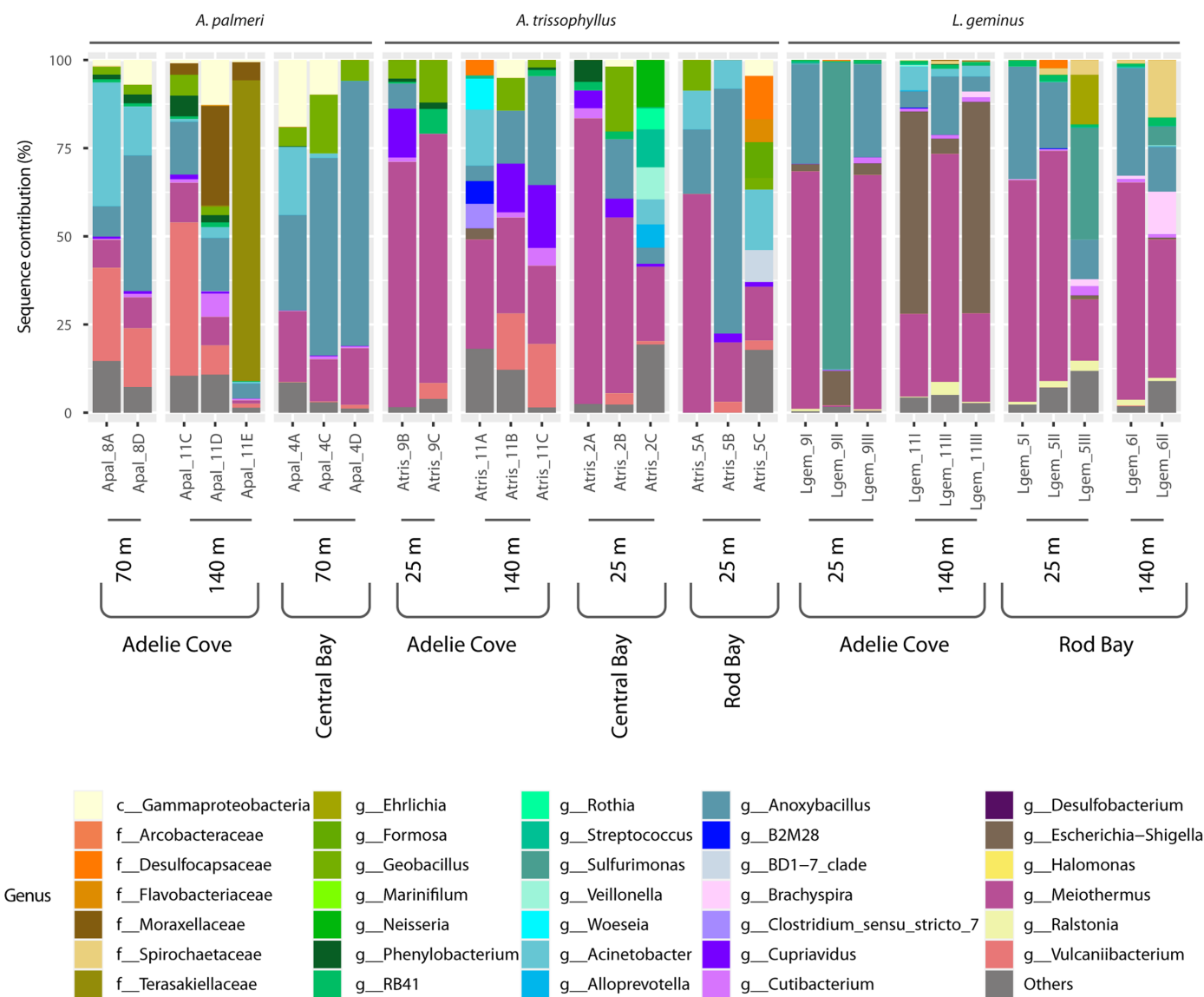


Fig. 2. Taxonomic composition of polychaete microbiomes. Bar plots showing the relative contribution (%) of bacterial taxa (at genus level when possible) associated with the three polychaetes species (*A. palmeri*, *A. trissophyllus*, and *L. geminus*) in the different areas (Adelie Cove, Central Bay, and Rod Bay) and depths (at 25, 70, and 140 m). All bacterial taxa with a relative abundance of less than 0.5% were grouped in "others."

composition ($P < 0.005$; fig. S8 and table S3). A dissimilarity of 97% was found, explained by the low contribution of *Meiothermus* and *Anoxybacillus* in the sediments (0.08% using the normalized dataset and 0.02% considering all the sequences obtained; fig. S13 and table S4). On the other hand, the main bacterial taxa of the sediments, *Blastopirellula* genus and Flavobacteraceae family, were present in only 20% of polychaetes specimens, with a contribution of less than 0.5% (except for Flavobacteraceae in two individuals of *A. trissophyllus*; 5% and 9%, respectively; Fig. 2). The results were further confirmed by the construction of the OTU bipartite network, which highlighted a very low number of OTUs (37 of the total 2025, corresponding to 1.8%; Fig. 3) shared between polychaetes and sediments. Similar results were also obtained after repeated ($n = 100$) rarefactions of the feature table to 1237 sequences (i.e.,

shared OTUs between polychaete and sediment microbiomes on average $3.2 \pm 0.2\%$).

Phylosymbiosis between polychaetes and microbiomes

A phylosymbiosis analysis was carried out to investigate whether microbial assemblages associated with Antarctic polychaetes maintained an ancient signal of host evolution. We found congruence between the 16S mitochondrial DNA-based phylogenetic tree of polychaetes and the microbiome diversity tree, inferred using the unweighted UniFrac dissimilarity and phylosymbiotic signals ($P < 0.05$, Mantel test; $P < 0.01$, Procrustes analysis) and were detected in a common ancestor between the two deposit feeders, *L. geminus* and *A. palmeri*, and an ancestor common to all three polychaete species (Fig. 4 and table S7).

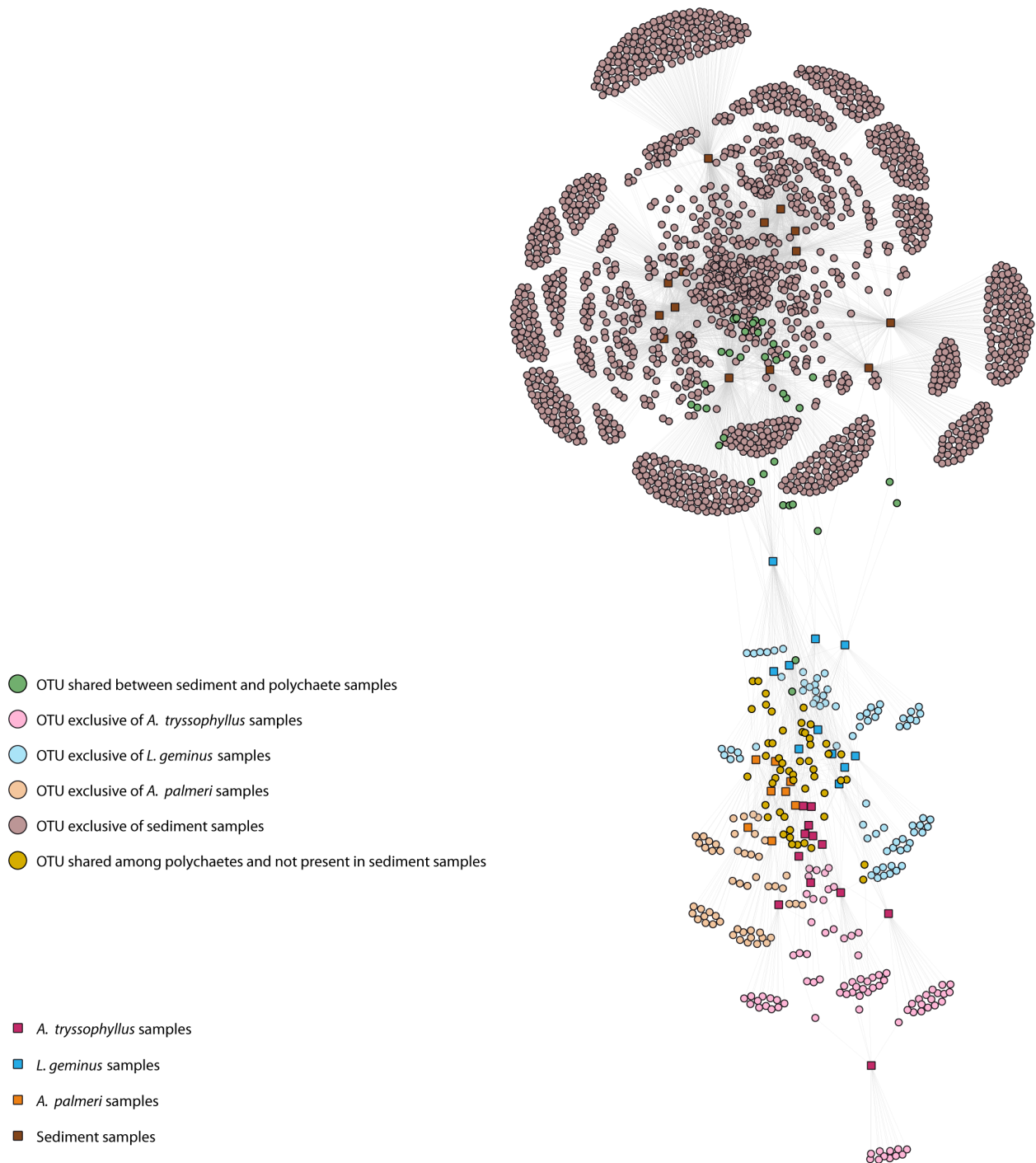


Fig. 3. OTU network of polychaete and sediment microbiomes. Network analysis showing the OTUs found in polychaete and sediment samples and relationships between them. Square nodes represent sample type (sediment or polychaete species), while round nodes represent OTUs; links between OTUs and samples are shown as gray lines. Sample nodes (squares) are colored according to the type/species: dark brown for sediments, light blue for *L. geminus*, purple for *A. trissophyllus*, and orange for *A. palmeri*. OTU nodes (circles) are colored according to their provenance: green for OTUs shared between sediments and polychaetes; yellow for OTUs exclusive of polychaetes; brown for OTUs exclusive of sediments; and pink, light blue, and orange for the OTUs exclusive of *A. trissophyllus*, *L. geminus*, and *A. palmeri* specimens, respectively.

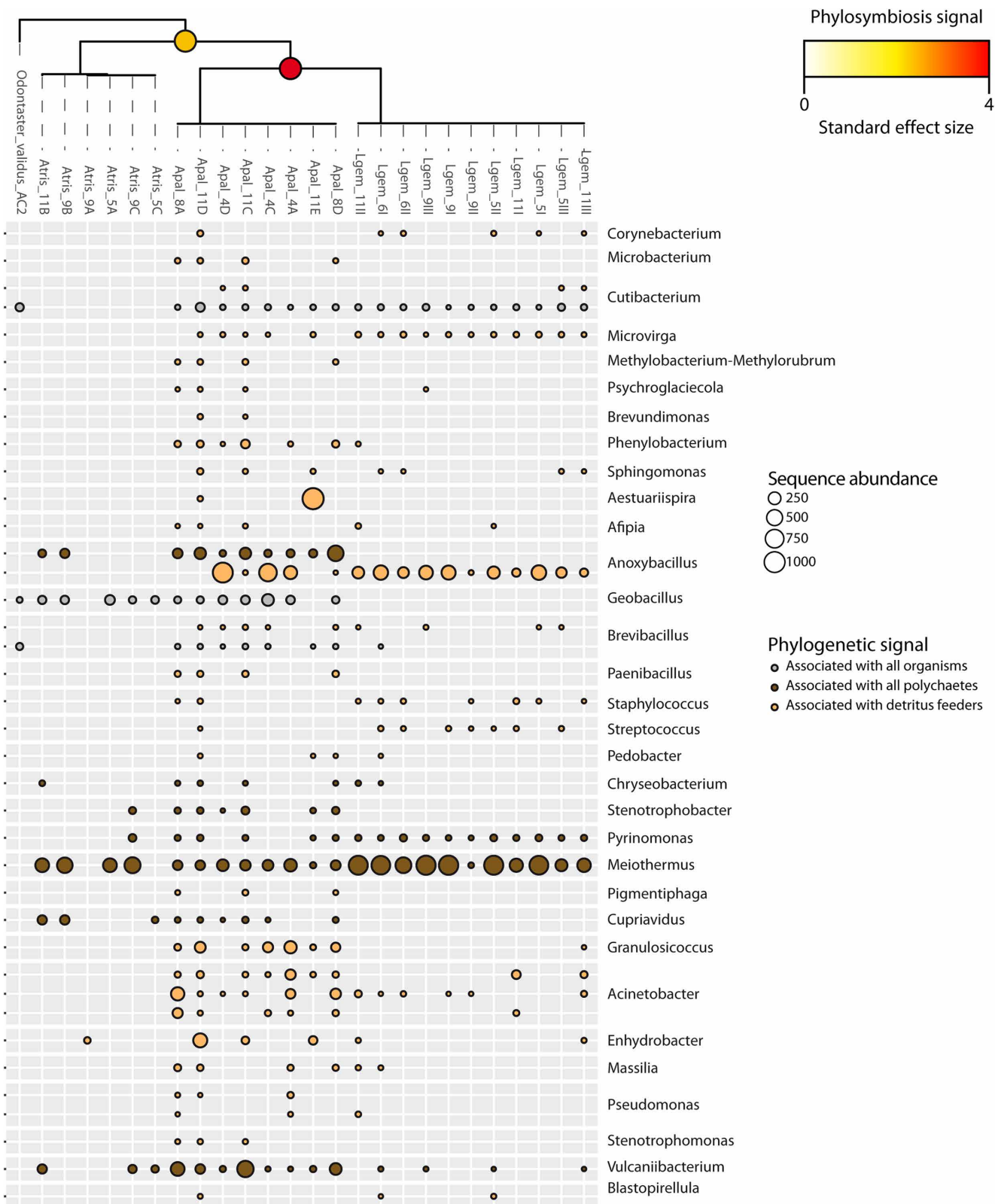


Fig. 4. Phyllosymbiosis signals in the polychaete microbiomes. The magnitude of the phyllosymbiotic signal along the host tree for each ancestor (the common ancestor between the two deposit feeders, the one common to all polychaetes, and the one also in common to the outgroup) was measured with a standard effect size per branch/node. Among all the OTUs found, only those that have shown a posterior probability of phyllosymbiosis up to 90% are shown in the figure, and their relative abundances are shown in each polychaete specimen. *O. validus* and its associated microbiome were used as an outgroup.

Among all the OTUs with a high phylosymbiotic signal, those that showed the maximum probability of phylosymbiosis (100%) and the highest relative abundances in all polychaete microbiomes were affiliated with *M. silvanus* (with the maximum signals in all polychaete species). Also, *A. flavithermus* showed maximum signals only in the ancestor of *L. geminus* and *A. palmeri* but not in the *A. trissophyllus* which was already phylogenetically separate from the detritivorous polychaetes (Fig. 4 and table S7).

Distribution of *Meiothermus* and *Anoxybacillus* and their genetic makeup for extremely cold conditions

The occurrence of *Meiothermus* and *Anoxybacillus* in the metagenomes of all annelid species available in gene banks was assessed through a 16S ribosomal DNA (rDNA) metabarcoding meta-analysis, while the genetic repertoire of these bacteria was investigated through a pangenomic approach. The metabarcoding meta-analysis revealed the lack of sequences related to the genera *Meiothermus* and *Anoxybacillus* in any other annelid microbiomes (table S8).

The analyses of the pangenomes of *Meiothermus* and *Anoxybacillus* (including 16 and 43 genomes, respectively) revealed the presence of genes coding for several functional traits potentially useful for coping with cold extreme conditions (see details on cold-related proteins in table S9). In particular, cold-shock proteins and ice-binding proteins encoded by the *CspLA* and *IbpB* genes for *Meiothermus* (94 and 75% of coverage, respectively) and the *CspD/CspB* and *IbpA* genes for *Anoxybacillus* (100 and 98% of coverage, respectively) were identified in almost all genomes investigated. Several genes related to acetyl-coenzyme A (CoA) metabolism and other alternative ways for energy generation (i.e., aldehyde dehydrogenase, alcohol dehydrogenase, and methylglyoxal synthase), as well as compounds and enzymes involved in osmo- and cryoprotection (i.e., glycine betaine, putrescine, spermidine, serine hydroxymethyltransferase, superoxide dismutase, acyl-CoA dehydrogenase, and enoyl-CoA hydratase), were also found in both *Meiothermus* and *Anoxybacillus* pangenomes with an average coverage of 87 and 91%, respectively (table S9). Other genes related to enzymes up-regulated during cold conditions such as phosphoenolpyruvate synthase, heterotetrameric sarcosine oxidase, and polyhydroxybutyrate were exclusively found in *Meiothermus* genomes (present in 69% of all genomes). Genes of ornithine and enzymes involved in propionyl-CoA metabolism were exclusively found in *Anoxybacillus* genomes (present in 99% of all genomes; table S9). The alignment-based analyses between OTUs of *Meiothermus* and *Anoxybacillus* associated with the microbiomes of the Antarctic polychaetes and the 16S rDNA obtained from the pangenomic analysis indicate an identity of 100% with *M. silvanus* strain VI-R2 and 99.43% with *A. flavithermus* strain 52-1A. The quantitative analysis of *Meiothermus* carried out through real-time quantitative polymerase chain reaction (PCR) revealed that the abundance of *Meiothermus* in the polychaete tissues ranged from $5.5 \pm 1.3 \times 10^5$ to $1.4 \pm 1.1 \times 10^7$ cells mg^{-1} dry weight.

Cryoprotective proteins in the microbiome of the Antarctic polychaetes

The results obtained from the proteomic analyses carried out on the total protein extracts from Antarctic polychaetes revealed the presence of several enzymes and proteins potentially useful for coping with extreme cold conditions (table S10). By matching untargeted

proteomic results with the specific UniProt databases, the identity of some proteins has been attributed exclusively to bacteria or polychaetes, and others are shared by both. In particular, the chaperone protein DnaK and the enzyme triosephosphate isomerase were identified and assigned to *Meiothermus*. Similarly, enzymes responsible for proline and glycerol production (i.e., glycerol-3-phosphate dehydrogenase and proline dehydrogenase), as well as enzymes involved in polysaccharide metabolism (i.e., 2-dehydro-3-deoxy-D-gluconate 5-dehydrogenase) and phenol degradation (i.e., 3-oxoadipate enol-lactonase), were assigned to *Meiothermus*. Moreover, proteins involved in other processes such as de novo synthesis of fatty acids (i.e., AcrR) and denitrification processes (i.e., NarL) were found and assigned to *Anoxybacillus*.

The results of Basic Local Alignment Search Tool for proteins (BLASTp) analyses carried out on proteins derived from proteomic analyses revealed a 100% identity (0 gaps, 3117 normalized bit-score) of the DnaK-matching sequence to the database entry D7BI94 (DnaK from *M. silvanus*).

To understand the biological relevance of the bacterial proteins identified, the fold change (FC) concerning the host constitutive proteins was calculated (see details in the Supplementary Materials). We found that this FC varied according to the constitutive proteins (40S ribosomal, 60S ribosomal, catalase, and histone H4) of the polychaetes. Bacterial triosephosphate isomerase, proline dehydrogenase, and 3-oxoadipate enol-lactonase showed the highest FC (1.61 to 5.52), whereas 2-dehydro-3-deoxy-D-gluconate 5-dehydrogenase the lowest FC (0.11 to 0.39) (Fig. 5 and table S11). Other cold-related proteins such as Heat Shock Protein 70 (HSP70), ubiquitin, peroxiredoxin, and thioredoxin attributed specifically to Antarctic polychaetes are reported in detail in table S10.

In silico analyses of physical-chemical properties of cold-related proteins

The results of in silico analysis of the physicochemical properties [defined using hydrophobicity and stability indices; sensu (32)] showed that 14 and 185 proteins produced by *Meiothermus* and *Anoxybacillus*, respectively, in different habitats worldwide have properties similar to those of known ice-related proteins (i.e., AFPs, ice binding, ice nucleating, and structuring proteins; fig. S14). Furthermore, among the extracted bacterial proteins from the Antarctic polychaetes, NarL (attributed to *Anoxybacillus*), 2-dehydro-3-deoxy-D-gluconate 5-dehydrogenase (assigned to *Meiothermus*), triosephosphate isomerase (assigned to *Meiothermus*), and DnaK (assigned to *M. silvanus*) showed physical-chemical properties typical of ice-related proteins (fig. S14).

DISCUSSION

Here, we provide evidence that dominant polychaetes endemic to Antarctic ecosystems (30, 31) live in close association with two genera of bacteria: *Meiothermus* and *Anoxybacillus*, which have never been reported in any other Antarctic invertebrate and annelid worldwide. All three polychaete species investigated in the Ross Sea, the two detritivorous *L. geminus* and *A. palmeri*, and the predator *A. trissophyllus*, shared the same microbiome core represented by the genera *Meiothermus* and *Anoxybacillus* (the latter not shared in all the specimens of *A. trissophyllus*), which largely prevailed over the others (i.e., contributing up to 70% of the microbiome). The microbiome core was not influenced by environmental factors as already

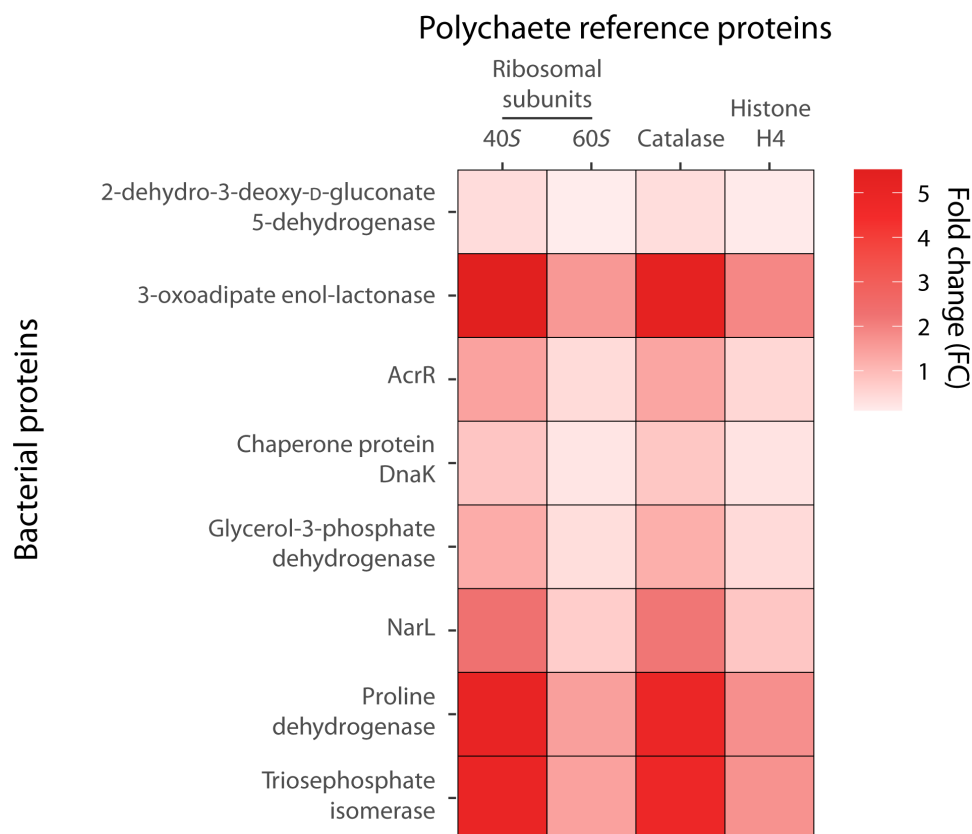


Fig. 5. Relative amount of bacterial cold-related proteins. The heatmap shows the FC of the bacterial proteins recovered by proteomic analysis, which was calculated by quantifying their relative signals compared to those of the polychaete's constitutive proteins (60S ribosomal protein, 40S ribosomal protein, catalase, and histone H4).

documented for other invertebrates on a global scale (7, 33). The same holds true for the microbiome of the predator *A. trissophyllus* and can be explained by the trophic independence of this polychaete from sedimentary organic detritus. *A. trissophyllus* is indeed a vagile carnivore, which feeds on small invertebrates (e.g., molluscs and crustaceans); therefore, other specific factors such as food sources could be determinants of its noncore bacteria (34, 35). These findings suggest that the bacterial core members of Antarctic polychaetes are driven by the biological interactions between hosts and associated bacteria.

Meiothermus bacteria are present at different latitudes in both marine and terrestrial ecosystems but typically at temperatures ranging from 40° to 60°C (36, 37). However, they have been reported also in subsurface polar habitats (38, 39). These chemoorgano-heterotrophs can produce thermostable polymers and enzymes degrading different organic substrates with high catalytic efficiency (36).

The *Anoxybacillus* genus (Bacillaceae family) has been identified in the gut of nonpolar marine organisms (40, 41) and marine geothermal habitats, including the Antarctic ones (42, 43). *Anoxybacillus* members are mostly thermophilic, anaerobic, and heterotrophic degraders of complex compounds (44) and are considered among the most “robust” bacteria on Earth due to their ability to produce endospores and thermostable molecules, thus providing high resistance to adverse conditions for prolonged periods (45, 46).

In the present study, quantitative analyses of *Meiothermus* cells in the polychaete tissues showed abundances similar or even higher than those found in other paradigmatic invertebrates such as in the mussel *Bathymodiolus* (up to 2.5×10^{12} in the entire body, $\sim 5 \times 10^6$ cells/mg of dry tissue) (47) and in the trophosome of the polychaete *Riftia pachyptila* (3.7×10^9 cells/g of fresh tissue, equivalent to $\sim 1.8 \times 10^7$ cells/mg of dry tissue) (48). These results expand previous literature information and provide evidence that *Meiothermus* and *Anoxybacillus* are present also in the tissues of marine organisms living in extremely cold conditions and not only in warmer conditions as previously reported.

The microbiome of Antarctic polychaetes was completely different from that of sediments. The dominant bacterial members of the sediments (*Blastopirellula* genus and Flavobacteriaceae family) were found only sporadically in polychaetes and with a negligible contribution (<1%). Similarly, the bacterial taxa identified in polychaetes, including *Meiothermus* and *Anoxybacillus*, were negligible in the sediments. A minor contribution of *Meiothermus* and *Anoxybacillus* was also observed in other investigations carried out in the Ross Sea and other polar marine ecosystems (42, 49, 50).

All these findings suggest that only a very small portion of bacteria belonging to *Meiothermus* and *Anoxybacillus* are now exchanged between the Antarctic polychaetes here investigated and the surrounding environment and vice versa.

The relevance of *Meiothermus* in subsuperficial sediments of the Ross ice shelf (15% of the total assemblage) indicates the importance

of these bacteria in past sediments (38), which allows us to hypothesize an ancient connection/exchange between these Antarctic polychaetes and this bacterial genus.

To evaluate whether microbial assemblages associated with Antarctic polychaetes maintain an ancient host evolution signal (18, 51), phylosymbiosis was investigated (18, 19). Phylosymbiosis has been observed in natural populations of marine invertebrates (12, 52), although this cannot be considered a general rule for marine metazoans (20). In our study, *Meiothermus* and *Anoxybacillus* (especially *M. silvanus* and *A. flavithermus*) showed the highest phylosymbiosis signals (100%) with the investigated Antarctic polychaetes. In particular, *Meiothermus* was involved in a close symbiotic relationship with all three polychaete species, while *Anoxybacillus* was phylogenetically closely related only with the detritivorous species (*L. geminus* and *A. palmeri*). This might suggest a different temporal pattern of association and transfer mode of *Anoxybacillus* by the predator *A. trissophyllus* compared to the detritivorous species being characterized not only by a divergent phylogenetic history but also by different biological traits (i.e., life cycle and reproduction and feeding behavior).

Although phylosymbiosis alone does not represent proof of coevolution and/or cospeciation between the host and microbiome nor vertical transmission (53, 54), the very high signals of phylosymbiosis observed in the present study contextual to the almost total absence of *Meiothermus* and *Anoxybacillus* in the present-day surface sediments strongly suggest a symbiosis arose in the past and perpetuated with vertical transmission.

The pangenomic analysis conducted in the present study on 59 *Meiothermus* and *Anoxybacillus* genomes available around the world showed that none of them was from cold environments, possibly due to the limited availability of studies focused on polar invertebrate microbiomes. Nonetheless, such analysis highlighted that *Meiothermus* and *Anoxybacillus* from different environments contain genes coding for several proteins (including enzymes) capable of ensuring metabolic functions and structural adaptations to extremely cold conditions. In particular, we found two ice-binding proteins in almost all the analyzed genomes of *Meiothermus* and *Anoxybacillus*, which are involved in preventing ice formation within cells and tissues and in lowering their freezing point (55). These results suggest that *Meiothermus* and *Anoxybacillus* associated with Antarctic polychaetes have a genetic repertoire that allows their survival in freezing conditions.

So far, studies on *Meiothermus* and *Anoxybacillus* have focused on their biotechnological applications and on research into their ability to degrade keratin (56), elastine (57), and starch (58). However, cocultivation of *Meiothermus* and *Anoxybacillus* appears essential to provide metabolic functions to other microorganisms (59), thus also supporting the evidence that the association between these two species with Antarctic polychaetes may be mutually beneficial.

Pioneer studies revealed that microorganisms themselves (60, 61) by acting as surfaces for the promotion of water molecule aggregation (62) may confer resistance to subzero temperatures (63). Other investigations on aquatic and terrestrial poikilothermic organisms hypothesized a connection between freeze tolerance and microbiome (64, 65). However, information on the role of the microbiome in the mechanisms adopted by marine invertebrates to cope with extreme cold and freezing conditions is limited.

In the present study, proteome analysis of Antarctic polychaetes revealed the presence of bacterial proteins in different tissues and

organs, including enzymes, with multiple cryoprotective functions. These bacterial proteins have been identified at quantitative levels comparable to or even higher than those of the polychaete's constitutive proteins. In particular, we recovered the DnaK chaperon protein, which was specifically assigned to *M. silvanus*. This protein has previously been reported to maintain proteostasis in bacteria living in cold environments (66). Furthermore, the enzyme triosephosphate isomerase assigned to *Meiothermus* was identified in the polychaete proteome. This enzyme has previously been found in other psychrophilic bacteria, and its role in adaptation to low temperatures has been documented (67). Among the proteins found in Antarctic polychaetes, AcrR, which was assigned to *Anoxybacillus*, has been reported to participate in fatty acid synthesis and membrane fluidity regulation (68). Other enzymes (i.e., glycerol-3-phosphate dehydrogenase and proline dehydrogenase) assigned to *Meiothermus* were found in the proteome of Antarctic polychaetes, such as those responsible for the production of proline and glycerol, which act as cryoprotectants in marine organisms due to their ability to reduce the freezing point of their internal liquids (69–72).

While DnaK, triosephosphate isomerase, and AcrR are bacterial proteins supporting directly microbial adaptation to cold habitats, the glycerol-3-phosphate dehydrogenase and proline dehydrogenase can contribute to the supply of key bacterial metabolites (e.g., proline and glycerol) that are ultimately absorbed and exploited by hosts to cope with the extreme conditions of Antarctic ecosystems.

Additional analyses also revealed that NarL (attributed to *Anoxybacillus*), 2-dehydro-3-deoxy-D-gluconate 5-dehydrogenase, triosephosphate isomerase, and DnaK showed physicochemical properties [in terms of stability and hydrophobicity; (32)] typical of known ice-related proteins (i.e., AFPs, ice binding, ice nucleating, and structuring proteins). In particular, the stability indices of the bacterial proteins identified in this study are among the highest observed for known ice-related proteins, thus suggesting a high efficiency of these proteins in contributing to the cryoprotection of the holobiont. Other proteins involved in cold resistance were exclusively attributed to the Antarctic polychaetes (e.g., HSP70, peroxiredoxin, and thioredoxin); thus, the contextual presence of proteins produced by *Meiothermus* and *Anoxybacillus* suggests a relevant contribution of the microbiome in the cryoprotection of the holobiont and its tolerance to extreme temperature conditions.

Overall, this study revealed that the microbiomes associated with three endemic Antarctic species of invertebrates have a stable bacterial core largely represented by *Meiothermus* and *Anoxybacillus* (although the latter only in deposit feeder polychaetes). These two taxa are characterized also by wide plasticity due to a versatile genetic makeup for different extreme temperature conditions, allowing them to produce enzymes and metabolites, which contribute to the portfolio of cryoprotective proteins of the holobiont (Fig. 6). Previous information documented the relevant presence of *Meiothermus* in the subsuperficial layers of the Ross Sea. Our analyses showed a close phylosymbiosis of *M. silvanus* and *A. flavithermus* with their hosts strongly suggesting the development of a stable and intimate and mutualistic relationship, which allowed the endemic Antarctic polychaetes and their microbiome to better adapt to the freezing temperatures (Fig. 6). The findings of this study open wider perspectives on the comprehension of the mechanisms of adaptation and cryo-resistance of marine invertebrates mediated by associated bacteria and pave the way for the development of biotechnological

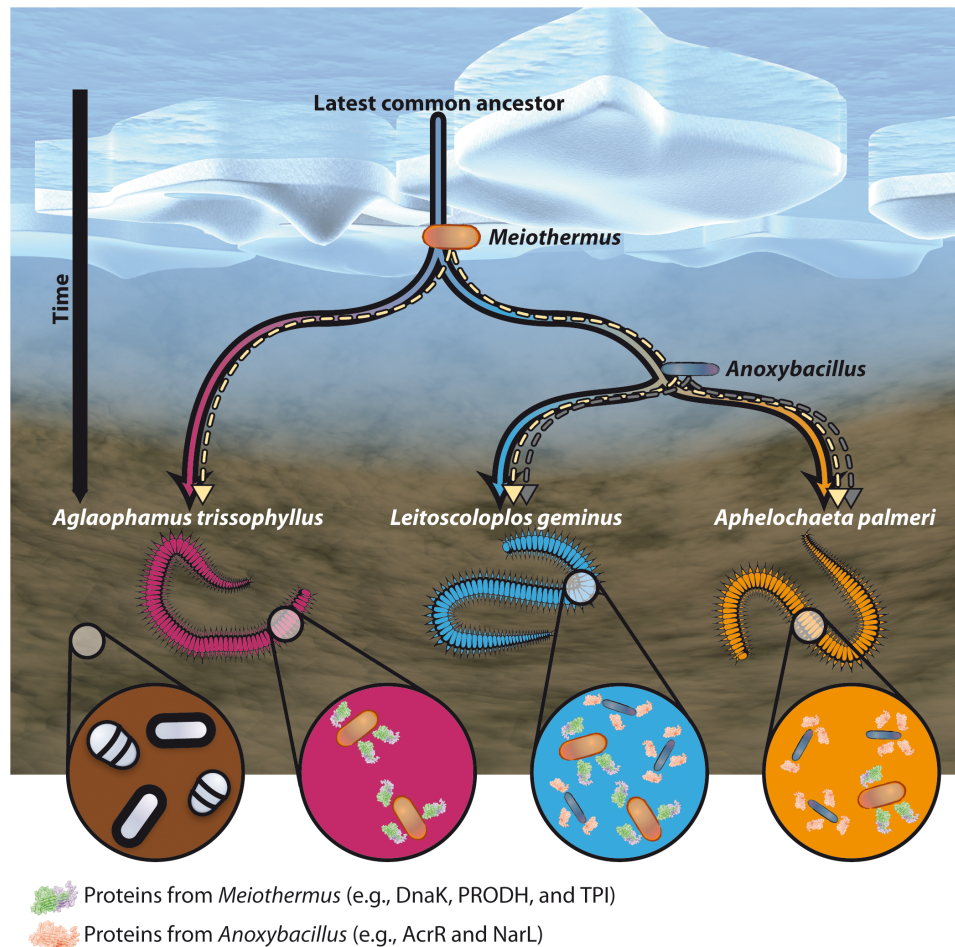


Fig. 6. Conceptual model illustrating the role of *Meiothermus* and *Anoxybacillus* in cryo-resistance of Antarctic polychaetes. The conceptual model shows the phyllosymbiosis relationships between *Meiothermus* and the three species of Antarctic polychaetes (the detritivorous *Aphelochaeta palmeri* and *Leitoscoloplos geminus* and the predator *Aglaophamus trissophyllus*) and between *Anoxybacillus* and the two detritivorous species. These bacteria are negligibly represented in the sediments, where other bacterial members thrive. The symbiosis between *Meiothermus* and/or *Anoxybacillus* has been perpetuated over time and allows the production of specific bacterial proteins such as DnaK, triosephosphate isomerase (TPI), and proline dehydrogenase (PRODH) (produced by *Meiothermus*) and AcrR, and NarL (produced by *Anoxybacillus*).

applications of the enzymes and molecules produced by *Meiothermus* and *Anoxybacillus* for cryo-preservation tools (73).

MATERIALS AND METHODS

Study design and sample collection

The Ross Sea is characterised by the largest continental shelf of Antarctica and is one of the most productive areas of the Southern Ocean. Here, we investigated the identity, origin, and proteome of the microbiota associated with three dominant endemic species of Antarctic polychaetes (*Leitoscoloplos geminus*, *Aphelochaeta palmeri*, and *Aglaophamus trissophyllus*; Fig. 1) and the factors influencing their structure, including phyllosymbiosis, to understand the role of the microbiome in the survival of marine invertebrates in the extreme conditions of Antarctic ecosystems. Sediment samples were collected through a Van Veen Grab (sampling surface, 0.18 m²), from three areas (hereafter defined as Adelie Cove, Rod Bay, and Central Bay; table S1 and fig. S1) in Terra Nova Bay, an inlet of about 64 km long on the eastern coast of the Ross Sea.

For each area, three independent deployments ($n = 3$) were made at three different increasing depths (25, 70, and 140 m). Each sediment sample was sieved through a metal sieve of 0.5-mm mesh, and macroinvertebrates, including polychaetes, were fixed in ethanol (95%) and identified morphologically under a stereomicroscope. Once identified, polychaetes were used for barcoding, microbiome metabarcoding, and proteomics.

Additional surface sediment samples (the top 10 cm) collected by three independent deployments were stored at -20°C for the analyses of microbiome, sedimentary grain size, and biochemical composition of organic matter. In addition, a conductivity-temperature-depth profile was carried out at each sampling depth of each area for temperature and salinity measurements. Additional details are reported in the Supplementary Materials.

Morphological identification of polychaetes

Morphological identification was carried out using specific dichotomous keys for Antarctic polychaete species (74–76). The polychaetes selected for this study based on their abundance and wide

distribution in the Antarctic ecosystems were *Aphelochaeta palmeri*, *Leitoscoloplos geminus*, and *Aglaophamus trissophyllus* (table S2 and Fig. 1). Hereinafter each specimen analyzed belonging to *L. geminus*, *A. palmeri*, and *A. trissophyllus* will be reported, respectively, as Lgem, Apal and Atris, followed by an identification code (table S2).

Molecular identification of the polychaetes

Total genomic DNA was extracted from a central body section (approximately 20 mg) of the polychaetes using the DNeasy Blood and Tissue Kit (Qiagen) and following the manufacturer's instructions with an incubation step with proteinase K at 56°C overnight. Genomic DNA quantification and quality control were performed with a NanoDrop 1000 Spectrophotometer (Thermo Fisher Scientific). To investigate the identity of specimens and their phylogenetic relationships, three mitochondrial markers were chosen and amplified: the coding mitochondrial *16S* and *12S* rRNA genes, selected for efficient species discrimination, and part of the mitochondrial protein-coding *COI* gene, a suitable fast-evolving barcoding gene, which exhibits a greater degree of genetic distance also at the intraspecific level, well-performing in the group of Polychaeta (31) (see details in the Supplementary Materials).

Polychaete phylogeny

Mitochondrial sequences obtained were analyzed using the software Geneious 7.1.9. Low-quality reading and primers sections were removed, and the two strands were assembled into consensus sequences. Multiple alignments were performed using the Multiple Sequence Comparison by Log-Expectation (MUSCLE) algorithm. All unique haplotypes were compared with sequences deposited in the public GenBank database (<http://ncbi.nlm.nih.gov/genbank/>) to validate the taxonomy of specimens and to find other sequences belonging to closely related species selected as additional ingroups or outgroups to build a more complete phylogenetic relationship among Antarctic polychaetes. Searches were performed using BLAST, verifying similarity with other known sequences (<https://blast.ncbi.nlm.nih.gov/>). Results with a low percentage of coverage (<90%) and a low percent identity (<95%) were not considered. Phylogenetic analyses were conducted in MEGA X (77) for all morphospecies investigated using the separated *16S*, *12S*, and *COI* datasets. The evolutionary history was inferred by using the maximum likelihood method applying the best-fit nucleotide substitution model: Hasegawa-Kishino-Yano for *16S* and *12S* and Tamura three-parameter for *COI* markers. An outgroup (*Sipunculus nudus*; KF042395.1, X96857.1, and FJ788920.1 for *16S*, *12S*, and *COI*, respectively) was added to better visualize the phylogenetic distances among samples.

Molecular analysis of the microbiome of the polychaetes and sediments

DNA was extracted from whole body tissues (~20 mg; including oral cavity, gut, parapodies, and teguments) of polychaetes. Furthermore, individuals belonging to *A. trissophyllus* (characterized by a size that allowed the separation of the different parts of the body) were also dissected, isolating the oral cavity, the gut, the parapodia, and the tegument (T). DNA was extracted from the different parts following the methods described above. Total genomic DNA was also extracted from different sediment aliquots (~1 g) from each deployment using the DNeasy PowerSoil Kit (Qiagen), following a modified protocol with initial treatment with three washing solutions

and 10-min incubation at 70°C, to achieve greater extraction efficiency. The DNA extracted from each sediment deployment was pooled before PCR amplification.

PCR amplification of an approximately 400-bp fragment of the bacterial *16S* rRNA gene (hypervariable regions V3 and V4) was carried out using the primer set 341F: (5'-CCTACGGGNGGCWGCAG-3') and 785R (5'-GACTACHVGGGTATCTAAKCC-3') (78). PCR products were purified and sequenced on an Illumina MiSeq sequencer using the V3 technology (2 × 300 bp) with the same primers used for the amplification, at LGC Genomics (see details in the Supplementary Materials).

Real-time quantitative analyses of the *16S* rDNA sequence belonging to the most abundant OTU of *Meiothermus* found in our samples through metabarcoding analyses are described in detail in the Supplementary Materials.

Bioinformatic analyses

Raw sequences were analyzed through the QIIME 2 pipeline (version 2022.2). Paired-end sequence files from each sequencing run were loaded, and sequence pairs were analyzed using the Divisive Amplicon Denoising Algorithm 2 (DADA2) plugin (79), which infers community composition in each sample by partitioning sequences according to the respective error models, thus filtering for erroneous reads and chimaeras and resolving minimal variations between prokaryotic taxa. Trimming parameters were set at 250 bp for forward-facing reads and 190 bp for reverse-facing reads. Paired sequences were then merged by the pipeline before producing an Amplicon Sequencing Variant table. Tables from separate runs were merged, and sequences were collapsed at 97% similarity to generate OTUs to avoid sequence duplication and lessen sparsity. Each sample was subsampled to 1237 sequences (minimum number of sequences obtained in the polychaete samples), thus obtaining a normalized OTU table. This approach was also used for the sediment microbiome analyses to allow a proper comparison with polychaete microbiomes. To assess the consistency of the results obtained, 100 random subsamples of the sediment microbiome sequences were performed. The normalization of the OTU table was used for the calculation of rarefaction curves and as input for the subsequent analyses, such as the determination of alpha and beta diversity indices (Shannon, Faith's phylogenetic diversity, Pielou's evenness, and OTU richness indices for alpha diversity and weighted and unweighted UniFrac distances for beta diversity). To infer the taxonomic assignment of OTUs, a taxonomic classifier was first trained on the small subunit (SSU) region amplified by the primers used in the present study on the SILVA reference database v138 and then used on the OTUs identified (80). The rarefied OTU table was visualized through a bipartite network using Cytoscape software (v3.9.1), to determine the proportions of bacterial OTUs shared between individual invertebrates and the surrounding sediments (20).

Phylosymbiosis analysis

To assess phylosymbiosis, we used microbiome compositions previously defined at the OTU level. One additional microbiome sample from a phylogenetically unrelated host inhabiting the same sediments (*Odontaster validus*) (81) was included in the dataset and used as an outgroup for the analysis. OTU taxonomic assignments were repeated using q2-feature-classifier (82) with the "top-hit" option on both the SILVA reference database v138 (80) and the Global Earth Microbiome database (83), to increase the likelihood of

successful assignment down to species level, when possible. Sequences assigned to chloroplasts, mitochondria, and Archaea, together with unassigned reads, were discarded. Last, we rarefied the OTU table to avoid biases owing to unequal sequencing depth across samples. Phylosymbiosis was first evaluated with a distance-based method by applying the Mantel test and Procrustes analysis to the distances retrieved from the host tree and the UniFrac compositional dissimilarities between microbiotas. Also, to better quantify the extent of the phylosymbiosis and identify the bacterial taxa contributing to the phylosymbiotic signal, we applied the same approach previously developed by Groussin and colleagues (84) (see details in the Supplementary Materials).

Metabarcoding meta-analysis and pangenomic-based approach

Further investigation was conducted to assess the distribution and potential roles of *Meiothermus* and *Anoxybacillus*. These genera were selected as they were the most abundant in the microbiomes of all polychaetes while almost exclusively absent in the sediment microbiomes and because they were characterized by a strong phylosymbiosis with the polychaete species (see Results).

Metabarcoding meta-analyses were first carried out on separate datasets on different species of Annelida to test whether OTUs belonging to both genera were found in other worm-associated metagenomes. We downloaded and analyzed (using the same approach on data produced in this work) data corresponding to four different projects available on National Center for Biotechnology Information (NCBI) exploring the diversity of annelid-associated prokaryotes in different environments (PRJNA171226, PRJNA438412, PRJNA497127, and PRJNA671766): *Ridgeia piscesae* at the Endeavour Hydrothermal Vents, *Oligobranchia haakonmosbiensis* within the Beaufort Sea, *Lamellibranchia barhami* and *Escarpia spicata* in the Gulf of California, and the anemone *Ostiactis pearseae* in association with chemosynthetic tubeworms in the Pescadero Basin (all found in hydrothermal vent areas). The resulting taxonomic table prepared using the same methods used for our samples (i.e., taxonomic classification on the SSU region amplified by the primers used in each study on the SILVA reference database v138) was then parsed to identify OTUs belonging to the genera of interest found in our work.

We also investigated the genetic repertoire of both *Meiothermus* and *Anoxybacillus* genera through a pangenome-based approach (85). The pangenome of *Meiothermus* comprised 16 genomes and that of *Anoxybacillus* 43 genomes (table S9). All available genomes were from hydrothermal vents, geothermal fluids, hot springs, and other habitats. Of all genomes in the data bank, none were available for polar environments.

The corresponding genomes were downloaded using the Bit Toolkit from the Genome Taxonomy Database (86) and further annotated using the Prokka tool. The results of the annotation were further parsed using the Pangenome Iterative Refinement and Threshold Evaluation (PIRATE) program to identify genes shared across the genomes of *Meiothermus* and *Anoxybacillus*. In particular, we searched the list of genes related to low-temperature adaptation, energy generation, fatty acid metabolism, mechanisms involved in stress resistance, and degradation of complex compounds (i.e., refractory fraction of organic matter, collagen, and chitin-like compounds; table S9); once a match was identified, the protein sequence corresponding to the gene listed was manually

checked through a BLASTp search on the NCBI database to ensure the correct gene identification.

The genomes gathered from the pangenomic analysis were also used to check for the taxonomic identification of the OTUs of *Meiothermus* and *Anoxybacillus*. This was carried out through pairwise alignments between the OTUs identified in our samples and the 16S rRNA genes extracted from the genomes using Multiple Alignment Based on Fast Fourier Transform (MAFFT) (87).

Metaproteomic analysis on the Antarctic polychaetes

Proteins were extracted from the whole body of a pool of *L. geminus* ($n = 5$) and *A. palmeri* ($n = 12$) individuals and a pool of *A. trissophyllus* individuals ($n = 5$) according to the protocol developed by Zhang and colleagues (88). Twenty microliters of the supernatant from each sample was subjected to SDS–polyacrylamide gel electrophoresis using precast 16.5% polyacrylamide gels (Bio-Rad). Details on electrophoresis and further steps of the procedure for protein extraction are reported in the Supplementary Materials. Micro liquid chromatography–high-resolution mass spectrometry (LC-HRMS) system was performed on an Eksigent M5 MicroLC system (Sciex) coupled to a TripleTOF 6600+ high-resolution mass spectrometer with OptiFlow Turbo V Ion Source (Sciex). In-gel digestion samples were analyzed in information-dependent acquisition mode. PepCal Mix (Sciex) assured steady MS and tandem MS (MS/MS) calibrations during the whole analysis timeframe. We processed the obtained data with ProteinPilot software (Sciex); Trypsin was set as a digestion enzyme and carbamidomethylation as a constant modification for cysteine. Matching was carried out against different UniProt Proteome databases (*Meiothermus* and *Anoxybacillus* and polychaeta) using Paragon Algorithm. Biological modification mode enabled to account for variable modifications of peptides. False discovery rate analysis was performed, and proteins with 95% confidence (unused score ≥ 1.3) were identified. FC of bacterial proteins found in Antarctic polychaetes was calculated by quantifying their LC-HRMS/MS signals against those of host constitutive proteins (60S ribosomal, 40S ribosomal, catalase, and histone H4; see details in the Supplementary Materials). Further, in silico analyses were carried out to compare the physico-chemical properties (in terms of hydrophobicity and stability) (32) of the proteins produced by *Meiothermus* and *Anoxybacillus* and those extracted in the present study, with the properties of known ice-related proteins (ice-binding, antifreeze, ice-nucleating, and ice-structuring proteins; see details in the Supplementary Materials).

Statistical analyses

Differences in the biochemical and grain size composition of sediments in the three different sampling areas and depths, as well as in the OTU richness, Shannon, Pielou's evenness, Faith's phylogenetic diversity values, and taxonomic composition of polychaete- and sediment-associated microbiomes, were assessed through a permutational analysis of variance. The following factors were considered: the area (fixed; three levels: Adelie Cove, Rod Bay, and Central Bay), the depth (nested in area; three levels: 25, 70, and 140 m), the species (fixed; three levels: *Leitoscoloplos*, *Aphelochaeta*, and *Aglaophamus*), and the source (fixed; two levels: polychaete and sediment). The factors area and depth (area) were tested within each polychaete species in the three areas of the Ross Sea where the individuals were present (table S3). Beta diversity was calculated among the different groups of samples (*L. geminus*, *A. palmeri*,

A. trissophyllus, and sediment) through weighted (considering both phylogenetic distances among OTUs and their abundances) and unweighted UniFrac distance (only considering phylogenetic distances among OTUs); the statistical significance of distances among sample groups calculated for each beta diversity index was assessed in the R environment using the *adonis2* function in the *vegan* R package with default values. A SIMPER analysis was performed to evaluate the percentages of similarity and/or dissimilarity in microbiome composition among specimens within each polychaete species (intraspecific variability), among the three polychaetes species (interspecific variability), and between polychaetes and sediments and to identify the main bacterial taxa responsible for differences. To investigate the potential contribution of environmental variables (i.e., temperature, salinity, depth, organic matter composition, and grain size) to the taxonomic composition of polychaete microbiomes, a distance-based linear model analysis was carried out for each polychaete species both in the whole microbiome, considering only the core microbiome (i.e., bacterial genera shared among all individuals within each polychaete species) and considering the microbiome excluding the core. Since some of the environmental variables are potentially correlated, for each dataset of each polychaete species, the presence of multicollinearity was investigated considering the areas and depth in which specimens were collected, through the Pearson correlation and the Variance Inflation Factors via Python (version 3.8.8). After this screening, only variables that did not display mutual correlation were considered in the analysis. All these analyses were performed with the PRIMER-E 6 software.

Supplementary Materials

This PDF file includes:

Supplementary Text

Figs. S1 to S14

Tables S1 and S2, S6 and S7, and S9 to S11

Legends for tables S3 to S5 and S8

References

Other Supplementary Material for this manuscript includes the following:

Tables S3 to S5 and S8

REFERENCES AND NOTES

1. M. McFall-Ngai, M. G. Hadfield, T. C. G. Bosch, H. V. Carey, T. Domazet-Lošo, A. E. Douglas, N. Dubilier, G. Eberl, T. Fukami, S. F. Gilbert, U. Hentschel, N. King, S. Kjelleberg, A. H. Knoll, N. Kremer, S. K. Mazmanian, J. L. Metcalf, K. Neelson, N. E. Pierce, J. F. Rawls, A. Reid, E. G. Ruby, M. Rumpho, J. G. Sanders, D. Tautz, J. J. Wernegreen, Animals in a bacterial world, a new imperative for the life sciences. *Proc. Natl. Acad. Sci. U.S.A.* **110**, 3229–3236 (2013).
2. F. J. Pollock, R. McMinds, S. Smith, D. G. Bourne, B. L. Willis, M. Medina, R. Vega Thurber, J. R. Zaneveld, Coral-associated bacteria demonstrate phylosymbiosis and cophylogeny. *Nat. Commun.* **9**, 4921 (2018).
3. A. Apprill, The role of symbioses in the adaptation and stress responses of marine organisms. *Ann. Rev. Mar. Sci.* **12**, 291–314 (2020).
4. S. R. Bordenstein, K. R. Theis, Host biology in light of the microbiome: Ten principles of holobionts and hologenomes. *PLoS Biol.* **13**, e1002226 (2015).
5. D. G. Bourne, K. M. Morrow, N. S. Webster, Insights into the coral microbiome: Underpinning the health and resilience of reef ecosystems. *Annu. Rev. Microbiol.* **70**, 317–340 (2016).
6. L. G. Wilkins, M. Leray, A. O’Dea, B. Yuen, R. S. Peixoto, T. J. Pereira, H. M. Bik, D. A. Coil, J. E. Duffy, E. A. Herre, H. A. Lessios, N. M. Lucey, L. C. Mejia, D. B. Rasher, K. H. Sharp, E. M. Sogin, R. W. Thacker, R. V. Thurber, W. T. Wcislo, E. G. Willbanks, J. A. Eisen, Host-associated microbiomes drive structure and function of marine ecosystems. *PLoS Biol.* **17**, e3000533 (2019).
7. O. Pantos, P. Bongaerts, P. G. Dennis, G. W. Tyson, O. Hoegh-Guldberg, Habitat-specific environmental conditions primarily control the microbiomes of the coral *Seriatopora hystrix*. *ISME J.* **9**, 1916–1927 (2015).
8. L. F. Lima, M. Weissman, M. Reed, B. Papudeshi, A. T. Alker, M. M. Morris, R. A. Edwards, S. J. de Putron, N. K. Vaidya, E. A. Dinsdale, Modeling of the coral microbiome: The influence of temperature and microbial network. *MBio* **11**, e02691-19 (2020).
9. E. S. Botté, S. Nielsen, M. A. A. Wahab, J. Webster, S. Robbins, T. Thomas, N. S. Webster, Changes in the metabolic potential of the sponge microbiome under ocean acidification. *Nat. Commun.* **10**, 4134 (2019).
10. T. J. Carrier, B. A. Leigh, D. J. Deaker, H. R. Devens, G. A. Wray, S. R. Bordenstein, M. Byrne, A. M. Reitzel, Microbiome reduction and endosymbiont gain from a switch in sea urchin life history. *Proc. Natl. Acad. Sci. U.S.A.* **118**, e2022023118 (2021).
11. A. T. Neu, E. E. Allen, K. Roy, Defining and quantifying the core microbiome: Challenges and prospects. *Proc. Natl. Acad. Sci. U.S.A.* **118**, e2104429118 (2021).
12. V. O. Ezenwa, N. M. Gerardo, D. W. Inouye, M. Medina, J. B. Xavier, Animal behavior and the microbiome. *Science* **338**, 198–199 (2012).
13. J. A. J. M. van de Water, D. Allemand, C. Ferrier-Pagès, Host-microbe interactions in octocoral holobionts—recent advances and perspectives. *Microbiome* **6**, 64 (2018).
14. B. F. R. de Oliveira, J. Freitas-Silva, C. Sánchez-Robinet, M. S. Laport, Transmission of the sponge microbiome: Moving towards a unified model. *Environ. Microbiol. Rep.* **12**, 619–638 (2020).
15. B. Koskella, J. Bergelson, The study of host–microbiome (co)evolution across levels of selection. *Philos. Trans. R. Soc. B Lond. B. Biol. Sci.* **375**, 20190604 (2020).
16. E. K. Mallott, K. R. Amato, Host specificity of the gut microbiome. *Nat. Rev. Microbiol.* **19**, 639–653 (2021).
17. L. P. Henry, M. Bruijning, S. K. G. Forsberg, J. F. Ayroles, The microbiome extends host evolutionary potential. *Nat. Commun.* **12**, 5141 (2021).
18. A. W. Brooks, K. D. Kohl, R. M. Brucker, E. J. van Opstal, S. R. Bordenstein, Phylosymbiosis: Relationships and functional effects of microbial communities across host evolutionary history. *PLoS Biol.* **14**, e2000225 (2016).
19. P. A. O’Brien, N. Andreakis, S. Tan, D. J. Miller, N. S. Webster, G. Zhang, Testing cophylogeny between coral reef invertebrates and their bacterial and archaeal symbionts. *Mol. Ecol.* **30**, 3768–3782 (2021).
20. V. Boscaro, C. C. Holt, N. W. L. Van Steenkiste, M. Herranz, N. A. T. Irwin, P. Álvarez-Campos, K. Grzelak, O. Holovachov, A. Kerbl, V. Mathur, N. Okamoto, R. S. Piercey, K. Worsaae, B. S. Leander, P. J. Keeling, Microbiomes of microscopic marine invertebrates do not reveal signatures of phylosymbiosis. *Nat. Microbiol.* **7**, 810–819 (2022).
21. K. L. Adair, A. E. Douglas, Making a microbiome: The many determinants of host-associated microbial community composition. *Curr. Opin. Microbiol.* **35**, 23–29 (2017).
22. S. L. Chown, A. Clarke, C. I. Fraser, S. Craig Cary, K. L. Moon, M. A. McGeoch, The changing form of Antarctic biodiversity. *Nature* **522**, 431–438 (2015).
23. L. S. Peck, Antarctic marine biodiversity: Adaptations, environments and responses to change, in *Oceanography and Marine Biology, Chapter 3* (CRC Press, ed. 1, 2018), p. 132.
24. C. L. Waller, M. R. Worland, P. Convey, D. K. A. Barnes, Ecophysiological strategies of Antarctic intertidal invertebrates faced with freezing stress. *Polar Biol.* **29**, 1077–1083 (2006).
25. W. Block, Cold tolerance of insects and other arthropods. *Philos. Trans. R. Soc. B* **326**, 613–633 (1990).
26. A. Boetius, A. M. Anesio, J. W. Deming, J. A. Mikucki, J. Z. Rapp, Microbial ecology of the cryosphere: Sea ice and glacial habitats. *Nat. Rev. Microbiol.* **13**, 677–690 (2015).
27. W. S. Shu, L. N. Huang, Microbial diversity in extreme environments. *Nat. Rev. Microbiol.* **20**, 219–235 (2022).
28. L. M. Herrera, C. X. García-Laviña, J. J. Marizcurrena, O. Volonterio, R. Ponce de León, S. Castro-Sowinski, Hydrolytic enzyme-producing microbes in the Antarctic oligochaete *Grania* sp. (Annelida). *Polar Biol.* **40**, 947–953 (2017).
29. M. S. Clark, L. S. Peck, HSP70 heat shock proteins and environmental stress in Antarctic marine organisms: A mini-review. *Mar. Genom.* **2**, 11–18 (2009).
30. G. Cantone, A. Castelli, M. C. Gambi, Benthic polychaetes off Terra Nova Bay and Ross Sea: Species composition, biogeography, and ecological role, in *Ross Sea Ecology* (Springer, 2000), pp. 551–561.
31. M. J. Brasier, H. Wiklund, L. Neal, R. Jeffreys, K. Linse, H. Ruhl, A. G. Glover, DNA barcoding uncovers cryptic diversity in 50% of deep-sea Antarctic polychaetes. *R. Soc. Open Sci.* **3**, 160432 (2016).
32. M. Bhattacharya, A. Hota, A. Kar, D. S. Chini, R. C. Malick, B. C. Patra, B. K. Das, In silico structural and functional modelling of Antifreeze protein (AFP) sequences of Ocean pout (*Zoarces americanus*, Bloch & Schneider 1801). *J. Genet. Eng. Biotechnol.* **16**, 721–730 (2018).
33. M. Lurgi, T. Thomas, B. Wemheuer, N. S. Webster, J. M. Montoya, Modularity and predicted functions of the global sponge-microbiome network. *Nat. Commun.* **10**, 992 (2019).
34. J. Tiede, C. Scherber, J. Mutschler, K. D. McMahon, C. Gratton, Gut microbiomes of mobile predators vary with landscape context and species identity. *Ecol. Evol.* **7**, 8545–8557 (2017).
35. L. Pita, L. Rix, B. M. Slaby, A. Franke, U. Hentschel, The sponge holobiont in a changing ocean: From microbes to ecosystems. *Microbiome* **6**, 46 (2018).
36. L. Albuquerque, M. S. da Costa, The family *Thermaceae*, in *The Prokaryotes* (Springer, 2014), pp. 955–987.

37. C. W. Herbold, C. K. Lee, I. R. McDonald, S. C. Cary, Evidence of global-scale aeolian dispersal and endemism in isolated geothermal microbial communities of Antarctica. *Nat. Commun.* **5**, 3875 (2014).
38. S. A. Carr, S. W. Vogel, R. B. Dunbar, J. Brandes, J. R. Spear, R. Levy, T. R. Naish, R. D. Powell, S. G. Wakeham, K. W. Mandernack, Bacterial abundance and composition in marine sediments beneath the Ross Ice Shelf, Antarctica. *Geobiology* **11**, 377–395 (2013).
39. Y. Blanco, O. Prieto-Ballesteros, M. J. Gómez, M. Moreno-Paz, M. García-Villadangos, J. A. Rodríguez-Manfredi, P. Cruz-Gil, M. Sánchez-Román, L. A. Rivas, V. Parro, Prokaryotic communities and operating metabolisms in the surface and the permafrost of Deception Island (Antarctica). *Environ. Microbiol.* **14**, 2495–2510 (2012).
40. T. D. Zeng, Y. Y. Pao, P. C. Chen, F. C. H. Weng, W. D. Jean, D. Wang, Effects of host phylogeny and habitats on gut microbiomes of oriental river prawn (*Macrobrachium nipponense*). *PLOS ONE* **10**, e0132860 (2015).
41. F. Naya-Català, G. do Vale Pereira, M. C. Piazzon, A. M. Fernandes, J. A. Caldusch-Giner, A. Sitjà-Bobadilla, L. E. C. Conceição, J. Pérez-Sánchez, Cross-talk between intestinal microbiota and host gene expression in gilthead sea bream (*Sparus aurata*) juveniles: Insights in fish feeds for increased circularity and resource utilization. *Front. Physiol.* **12**, 748265 (2021).
42. A. G. Bendia, G. G. Araujo, A. A. Pulschen, B. Contro, R. T. D. Duarte, F. Rodrigues, D. Galante, V. H. Pellizari, Surviving in hot and cold: Psychrophiles and thermophiles from Deception Island volcano, Antarctica. *Extremophiles* **22**, 917–929 (2018).
43. J. Schultz, M. T. D. Parise, D. Parise, L. G. Medeiros, T. J. Sousa, R. B. Kato, A. P. T. Uetanabaro, F. Araújo, R. T. J. Ramos, S. de Castro Soares, B. Brenig, V. A. de Carvalho Azevedo, A. Góes-Neto, A. S. Rosado, Unraveling the genomic potential of the thermophilic bacterium *Anoxybacillus flavithermus* from an antarctic geothermal environment. *Microorganisms* **10**, 1673 (2022).
44. G. Chen, X. An, L. Feng, X. Xia, Q. Zhang, Genome and transcriptome analysis of a newly isolated azo dye degrading thermophilic strain *Anoxybacillus* sp. *Ecotoxicol. Environ. Saf.* **203**, 111047 (2020).
45. I. Mandic-Mulec, P. Stefanic, J. van Elsland, Ecology of *Bacillaceae*, in *The Bacterial Spore: From Molecules to Systems* (ASM Press, 2016).
46. S. V. D. Reis, W. O. Beys-da-Silva, L. Tironi, L. Santi, A. Seixas, C. Termignoni, M. V. da Silva, A. J. Macedo, The extremophile *Anoxybacillus* sp. PC2 isolated from Brazilian semiarid region (Caatinga) produces a thermostable keratinase. *J. Basic Microbiol.* **60**, 809–815 (2020).
47. S. Duperron, A. Quiles, K. M. Szafranski, N. Leger, B. Shillito, Estimating symbiont abundances and gill surface areas in specimens of the hydrothermal vent mussel *Bathymodiolus puteoserpentis* maintained in pressure vessels. *Front. Mar. Sci.* **3**, 16 (2016).
48. C. M. Cavanaugh, S. L. Gardiner, M. L. Jones, H. W. Jannasch, J. B. Waterbury, Prokaryotic cells in the hydrothermal vent tube worm *Riftia pachyptila* Jones: Possible chemoautotrophic symbionts. *Science* **213**, 340–342 (1981).
49. C. Martínez-Pérez, C. Greening, S. K. Bay, R. J. Lappan, Z. Zhao, D. De Corte, C. Hulbe, C. Ohnheiser, C. Stevens, B. Thomson, R. Stepanauskas, J. M. González, R. Logares, G. J. Herndl, S. E. Morales, F. Baltar, Phylogenetically and functionally diverse microorganisms reside under the Ross Ice Shelf. *Nat. Commun.* **13**, 117 (2022).
50. A. Jain, K. P. Krishnan, Differences in free-living and particle-associated bacterial communities and their spatial variation in Kongsfjorden, Arctic. *J. Basic Microbiol.* **57**, 827–838 (2017).
51. S. J. Lim, S. R. Bordenstein, An introduction to phylosymbiosis. *Proc. R. Soc. B* **287**, 20192900 (2020).
52. C. G. Easson, R. W. Thacker, Phylogenetic signal in the community structure of host-specific microbiomes of tropical marine sponges. *Front. Microbiol.* **5**, 532 (2014).
53. F. Mazel, K. M. Davis, A. Loudon, W. K. Kwong, M. Groussin, L. W. Parfrey, Is host filtering the main driver of phylosymbiosis across the tree of life? *Msystems* **3**, 10–1128 (2018).
54. K. H. Sharp, D. Distel, V. J. Paul, Diversity and dynamics of bacterial communities in early life stages of the Caribbean coral *Porites astreoides*. *ISME J.* **6**, 790–801 (2012).
55. M. Bar Dolev, I. Braslavsky, P. L. Davies, Ice-binding proteins and their function. *Annu. Rev. Biochem.* **85**, 515–542 (2016).
56. J. M. Kuo, J. I. Yang, W. M. Chen, M. H. Pan, M. L. Tsai, Y. J. Lai, A. Hwang, B. S. Pan, C. Y. Lin, Purification and characterization of a thermostable keratinase from *Meiothermus* sp. I40. *Int. Biodeter. Biodegr.* **70**, 111–116 (2012).
57. T. Matsui, Y. Yamada, H. Mitsuya, Y. Shigeri, Y. Yoshida, Y. Saito, H. Matsui, K. Watanabe, Sustainable and practical degradation of intact chicken feathers by cultivating a newly isolated thermophilic *Meiothermus ruber* H328. *Appl. Microbiol. Biotechnol.* **82**, 941–950 (2009).
58. A. Poli, E. Esposito, L. Lama, P. Orlando, G. Nicolaus, F. De Appolonia, A. Gambacorta, B. Nicolaus, *Anoxybacillus amylolyticus* sp. nov., a thermophilic amylase producing bacterium isolated from Mount Rittmann (Antarctica). *Syst. Appl. Microbiol.* **29**, 300–307 (2006).
59. M. Tank, D. A. Bryant, Nutrient requirements and growth physiology of the photoheterotrophic Acidobacterium, *Chloracidobacterium thermophilum*. *Front. Microbiol.* **6**, 226 (2015).
60. C. J. Klok, S. L. Chown, Critical thermal limits, temperature tolerance and water balance of a sub-Antarctic caterpillar, *Pringleophaga marioni* (Lepidoptera: Tineidae). *J. Insect Physiol.* **43**, 685–694 (1997).
61. M. R. Worland, W. Block, Ice-nucleating bacteria from the guts of two sub-antarctic beetles, *Hydromedion sparsutum* and *Perimylops antarcticus* (Perimylopidae). *Cryobiology* **38**, 60–67 (1999).
62. J. S. Bale, Insects and low temperatures: From molecular biology to distributions and abundance. *Philos. Trans. R. Soc. B* **357**, 849–862 (2002).
63. M. J. Everatt, P. Convey, J. S. Bale, M. R. Worland, S. A. Hayward, Responses of invertebrates to temperature and water stress: A polar perspective. *J. Therm. Biol.* **54**, 118–132 (2015).
64. F. Kokou, G. Sasson, T. Nitzan, A. Doron-Faigenboim, S. Harpaz, A. Cnaani, I. Mizrahi, Host genetic selection for cold tolerance shapes microbiome composition and modulates its response to temperature. *eLife* **7**, e36398 (2018).
65. M. Morgan-Richards, C. J. Marshall, P. J. Biggs, S. A. Treweek, Insect freeze-tolerance Downunder: The microbial connection. *Insects* **14**, 89 (2023).
66. N. J. Maillot, F. A. Honoré, D. Byrne, V. Méjean, O. Genest, Cold adaptation in the environmental bacterium *Shewanella oneidensis* is controlled by a J-domain co-chaperone protein network. *Commun. Biol.* **2**, 323 (2019).
67. J. Åqvist, Cold adaptation of triosephosphate isomerase. *Biochemistry* **56**, 4169–4176 (2017).
68. Q. Yang, Y. Shi, Y. Xin, T. Yang, L. Zhang, Z. Gu, Y. Li, Z. Ding, G. Shi, Insight into the cold adaptation mechanism of an aerobic denitrifying bacterium: *Bacillus simplex* H-b. *Appl. Environ. Microbiol.* **89**, e01928-22 (2023).
69. J. A. Raymond, Glycerol is a colligative antifreeze in some northern fishes. *J. Exp. Zool.* **262**, 347–352 (1992).
70. K. V. Ewart, A. E. Fletcher, The role of glycerol as a cryoprotectant in Antarctic fishes. *J. Comp. Physiol. B* **156**, 619–630 (1986).
71. K. E. Zachariassen, E. Kristiansen, Ice nucleation and antinucleation in nature. *Cryobiology* **41**, 257–279 (2000).
72. Y. Zhang, Z. Chen, Y. Wang, H. Dong, J. Sun, J. Li, X. Mao, Molecular modelling studies reveal cryoprotective mechanism of L-Proline during the frozen storage of shrimp (*Litopenaeus vannamei*). *Food Chem.* **441**, 138259 (2024).
73. J. Yang, L. Gao, M. Liu, X. Sui, Y. Zhu, C. Wen, L. Zhang, Advanced biotechnology for cell cryopreservation. *Tianjin Univ.* **26**, 409–423 (2020).
74. J. A. Blake, Polychaeta Orbinidae from Antarctica, the Southern Ocean, the Abyssal Pacific Ocean, and off South America. *Zootaxa* **4218**, 1–145 (2017).
75. J. A. Blake, Bitentaculate Cirratulidae (Annelida, Polychaeta) collected chiefly during cruises of the R/V Anton Bruun, USNS Eltanin, USCG Glacier, R/V Hero, RVIB Nathaniel B. Palmer, and R/V Polarstern from the Southern Ocean, Antarctica, and off Western South America. *Zootaxa* **4537**, 1–130 (2018).
76. G. A. Knox, D. B. Cameron, *The Marine Fauna of the Ross Sea: Polychaeta* (NIWA Biodiversity Publisher, 1998).
77. S. Kumar, G. Stecher, M. Li, C. Knyaz, K. Tamura, MEGA X: Molecular evolutionary genetics analysis across computing platforms. *Mol. Biol. Evol.* **35**, 1547–1549 (2018).
78. A. Klindworth, E. Pruesse, T. Schweer, J. Peplies, C. Quast, M. Horn, F. O. Glöckner, Evaluation of general 16S ribosomal RNA gene PCR primers for classical and next-generation sequencing-based diversity studies. *Nucleic Acids Res.* **41**, e1 (2013).
79. B. J. Callahan, P. J. McMurdie, M. J. Rosen, A. W. Han, A. Jo, A. Johnson, S. P. Holmes, DADA2: High-resolution sample inference from Illumina amplicon data. *Nat. Methods* **13**, 581–583 (2016).
80. C. Quast, E. Pruesse, P. Yilmaz, J. Gerken, T. Schweer, P. Yarza, J. Peplies, F. O. Glöckner, The SILVA ribosomal RNA gene database project: Improved data processing and web-based tools. *Nucleic Acids Res.* **41**, D590–D596 (2012).
81. E. Buschi, A. Dell'Anno, M. Tangherlini, S. Stefanni, M. L. Martire, L. Núñez-Pons, A. Conxita, C. Corinaldesi, Rhodobacteraceae dominate the core microbiome of the sea star *Odontaster validus* (Koehler, 1906) in two opposite geographical sectors of the Antarctic Ocean. *Front. Microbiol.* **14**, 1234725 (2023).
82. N. A. Bokulich, B. D. Kaehler, J. R. Rideout, M. Dillon, E. Bolyen, R. Knight, G. A. Huttley, J. G. Caporaso, Optimizing taxonomic classification of marker-gene amplicon sequences with QIIME 2's q2-feature-classifier plugin. *Microbiome* **6**, 90 (2018).
83. S. Nayfach, S. Roux, R. Seshadri, D. Udwaray, N. Varghese, F. Schulz, D. Wu, D. Paez-Espino, I. M. Chen, M. Hüntemann, K. Palaniappan, J. Ladau, S. Mukherjee, T. B. K. Reddy, T. Nielsen, E. Kirton, J. P. Faria, J. N. Edirisinghe, C. S. Henry, S. P. Jungbluth, D. Chivian, P. Dehal, E. M. Wood-Charlson, A. P. Arkin, S. G. Tringe, A. Visel, IMG/M Data Consortium, T. Woyke, N. J. Mouncey, N. N. Ivanova, N. C. Kyrpides, E. A. Elze-Fadrosh, Show fewer authors A genomic catalog of Earth's microbiomes. *Nat. Biotechnol.* **39**, 499–509 (2021).
84. M. F. Groussin, J. G. Mazel, C. S. Sanders, S. Smillie, W. Lavergne, E. J. Thuiller, Alm, Unraveling the processes shaping mammalian gut microbiomes over evolutionary time. *Nat. Commun.* **8**, 14319 (2017).
85. E. Bosi, M. Fondi, V. Orlandini, E. Perrin, I. Maida, D. de Pascale, M. L. Tutino, E. Parrilli, A. Lo Giudice, A. Filloux, R. Fani, The pangenome of (Antarctic) *Pseudoalteromonas* bacteria: Evolutionary and functional insights. *BMC Genomics* **18**, 93 (2017).

86. D. H. Parks, M. Chuvochina, C. Rinke, A. J. Mussig, P. A. Chaumeil, P. Hugenholtz, GTDB: An ongoing census of bacterial and archaeal diversity through a phylogenetically consistent, rank normalized and complete genome-based taxonomy. *Nucleic Acids Res.* **50**, 785–794 (2021).
87. K. Katoh, D. M. Standley, MAFFT: Iterative refinement and additional methods. *Methods Mol. Biol.* **1079**, 131–146 (2014).
88. Y. Zhang, J. Sun, K. Xiao, S. M. Arellano, V. Thiyagarajan, P. Y. Qian, 2D gel-based multiplexed proteomic analysis during larval development and metamorphosis of the biofouling polychaete tubeworm *Hydroides elegans*. *J. Proteome Res.* **9**, 4851–4860 (2010).
89. P. Convey, L. S. Peck, Antarctic environmental change and biological responses. *Sci. Adv.* **5**, eaaz0888 (2019).
90. F. Semprucci, L. Appolloni, E. Grassi, L. Donnarumma, L. Cesaroni, G. Tirimberio, E. Chianese, P. Di Donato, G. F. Russo, M. Balsamo, R. Sandulli, Antarctic special protected area 161 as a reference to assess the effects of anthropogenic and natural impacts on meiobenthic assemblages. *Diversity* **13**, 626 (2021).
91. S. D. Emslie, Ancient Adélie penguin colony revealed by snowmelt at Cape Irizar, Ross Sea, Antarctica. *Geology* **49**, 145–149 (2021).
92. R. Danovaro, *Methods for the Study of Deep-Sea Sediments, their Functioning and Biodiversity* (CRC Press, ed. 1, 2009).
93. I. Bertocci, A. Dell'Anno, L. Musco, C. Gambi, V. Saggiomo, M. Cannavacciuolo, M. Lo Martire, A. Passarelli, G. Zazo, R. Danovaro, Multiple human pressures in coastal habitats: Variation of meiofaunal assemblages associated with sewage discharge in a post-industrial area. *Sci. Total Environ.* **655**, 1218–1231 (2019).
94. C. J. Lorenzen, S. W. Jeffrey, Determination of chlorophyll and phaeopigments spectrophotometric equations. *Limnol. Oceanogr.* **12**, 343–346 (1980).
95. A. Pusceddu, A. Dell'Anno, M. Fabiano, R. Danovaro, Quantity and bioavailability of sediment organic matter as signatures of benthic trophic status. *Mar. Ecol. Prog. Ser.* **375**, 41–52 (2009).
96. A. Pusceddu, A. Dell'Anno, M. Fabiano, Organic matter composition in coastal sediments at Terra Nova Bay (Ross Sea) during summer 1995. *Polar Biol.* **2**, 288–293 (2000).
97. E. Sjölin, C. Erséus, M. Källersjö, Phylogeny of Tubificidae (Annelida, Clitellata) based on mitochondrial and nuclear sequence data. *Mol. Phylogenet. Evol.* **35**, 431–441 (2005).
98. P. Trontelj, S. Y. Utevsy, Celebrity with a neglected taxonomy: Molecular systematics of the medicinal leech (genus *Hirudo*). *Mol. Phylogenet. Evol.* **34**, 616–624 (2005).
99. O. Folmer, M. Black, W. Hoeh, R. Lutz, R. Vrijenhoek, DNA primers for amplification of mitochondrial cytochrome c oxidase subunit I from diverse metazoan invertebrates. *Marine Biotechnol.* **3**, 294–299 (1994).
100. F. Sanger, S. Nicklen, A. R. Coulson, DNA sequencing with chain-terminating inhibitors. *PNAS* **74**, 5463–5467 (1977).
101. J. Einen, I. H. Thorseth, L. Øvreås, Enumeration of Archaea and Bacteria in seafloor basalt using real-time quantitative PCR and fluorescence microscopy. *FEMS Microbiol. Lett.* **282**, 182–187 (2008).
102. M. Csűös, Count: Evolutionary analysis of phylogenetic profiles with parsimony and likelihood. *Bioinformatics* **26**, 1910–1912 (2010).
103. N. J. Gotelli, Null model analysis of species co-occurrence patterns. *Ecology* **81**, 2606–2621 (2000).
104. A. Shevchenko, H. Tomas, J. Havli, J. V. Olsen, M. Mann, In-gel digestion for mass spectrometric characterization of proteins and proteomes. *Nat. Protoc.* **1**, 2856–2860 (2006).
105. E. Gasteiger, C. Hoogland, A. Gattiker, S. E. Duvaud, M. R. Wilkins, R. D. Appel, A. Bairoch, Protein identification and analysis tools on the ExPASy server, in *The Proteomics Protocols Handbook*. Springer Protocols Handbooks, J. M. Walker, Ed. (Humana Press, 2005), pp. 571–607.
106. H. L. Ayala-del-Río, P. S. Chain, J. J. Grzymalski, M. A. Ponder, N. Ivanova, P. W. Bergholz, G. Di Bartolo, L. Hauser, M. Land, C. Bakermans, D. Rodrigues, J. Klappenbach, D. Zarka, F. Larimer, P. Richardson, A. Murray, M. Thomashow, J. M. Tiedje, The genome sequence of *Psychrobacter arcticus* 273-4, a psychrotolerant Siberian permafrost bacterium, reveals mechanisms for adaptation to low-temperature growth. *Appl. Environ. Microbiol.* **76**, 2304–2312 (2010).
107. H. Y. Koh, H. Park, J. H. Lee, S. J. Han, Y. C. Sohn, S. G. Lee, Proteomic and transcriptomic investigations on cold-responsive properties of the psychrophilic Antarctic bacterium *Psychrobacter* sp. PAMC 21119 at subzero temperatures. *Environ. Microbiol.* **19**, 628–644 (2017).
108. D. F. Rodrigues, J. M. Tiedje, Coping with our cold planet. *Appl. Environ. Microbiol.* **74**, 1677–1686 (2008).
109. H. Aliyu, P. De Maayer, D. Cowan, The genome of the Antarctic polyextremophile *Nesterenkonia* sp. AN1 reveals adaptive strategies for survival under multiple stress conditions. *FEMS Microbiol. Ecol.* **92**, fiv032 (2016).
110. N. C. S. Mykityczuk, J. R. Lawrence, C. R. Omelon, L. G. Whyte, Microscopic characterization of the bacterial cell envelope of *Planococcus halocryophilus* Or1 during subzero growth at –15 °C. *Polar Biol.* **39**, 701–712 (2016).
111. P. M. Tribelli, E. C. S. Venero, M. M. Ricardi, M. Gómez-Lozano, L. J. R. Iustman, S. Molin, N. I. López, Novel essential role of ethanol oxidation genes at low temperature revealed by transcriptome analysis in the Antarctic bacterium *Pseudomonas extremaustralis*. *PLOS ONE* **10**, e0145353 (2015).
112. L. Ting, T. J. Williams, M. J. Cowley, F. M. Lauro, M. Guilhaus, M. J. Raftery, R. Cavicchioli, Cold adaptation in the marine bacterium, *Sphingopyxis alaskensis*, assessed using quantitative proteomics. *Environ. Microbiol.* **12**, 2658–2676 (2010).
113. H. Koo, J. A. Hakim, P. R. E. Fisher, A. Grueneberg, D. T. Andersen, A. K. Bej, Distribution of cold adaptation proteins in microbial mats in Lake Joyce, Antarctica: Analysis of metagenomic data by using two bioinformatics tools. *J. Microbiol. Methods* **120**, 23–28 (2016).
114. P. Fonseca, R. Moreno, F. Rojo, Growth of *Pseudomonas putida* at low temperature: Global transcriptomic and proteomic analyses. *Environ. Microbiol. Rep.* **3**, 329–339 (2011).
115. A. R. Horswill, J. C. Escalante-Semerena, *Salmonella typhimurium* LT2 catabolizes propionate via the 2-methylcitric acid cycle. *J. Bacteriol.* **181**, 5615–5623 (1999).
116. R. E. Collins, J. W. Deming, An inter-order horizontal gene transfer event enables the catabolism of compatible solutes by *Colwellia psychrerythraea* 34H. *Extremophiles* **17**, 601–610 (2013).
117. S. Mocali, C. Chiellini, A. Fabiani, S. Decuzzi, D. de Pascale, E. Parrilli, M. L. Tutino, E. Perrin, E. Bosi, M. Fondi, A. Lo Giudice, R. Fani, Ecology of cold environments: New insights of bacterial metabolic adaptation through an integrated genomic-phenomic approach. *Sci. Rep.* **7**, 839 (2017).
118. A. Tkachenko, L. Nesterova, M. Pshenichnov, The role of the natural polyamine putrescine in defense against oxidative stress in *Escherichia coli*. *Arch. Microbiol.* **176**, 155–157 (2001).
119. X. Zhu, Q. Li, J. Hu, M. Wang, X. Li, Molecular cloning and characterization of spermine synthase gene associated with cold tolerance in tea plant (*Camellia sinensis*). *Appl. Biochem. Biotechnol.* **177**, 1055–1068 (2015).
120. G. V. Smirnova, O. N. Zakirova, O. N. Oktyabrskii, The role of antioxidant systems in the cold stress response of *Escherichia coli*. *Microbiol.* **70**, 45–50 (2001).
121. R. Margesin, V. Miteva, Diversity and ecology of psychrophilic microorganisms. *Res. Microbiol.* **162**, 346–361 (2011).
122. B. A. Methé, K. E. Nelson, J. W. Deming, B. Momen, E. Melamud, X. Zhang, J. Moulton, R. T. DeBoy, J. F. Kolonay, S. A. Sullivan, L. Zhou, T. M. Davidsen, M. Wu, A. L. Huston, M. Lewis, B. Weaver, J. F. Weidman, H. Khouri, T. R. Utterback, T. V. Feldblyum, C. M. Fraser, The psychrophilic lifestyle as revealed by the genome sequence of *Colwellia psychrerythraea* 34H through genomic and proteomic analyses. *Proc. natl. Acad. Sci. U.S.A.* **102**, 10913–10918 (2005).
123. M. V. Catone, J. A. Ruiz, M. Castellanos, D. Segura, G. Espin, N. I. López, High polyhydroxybutyrate production in *Pseudomonas extremaustralis* is associated with differential expression of horizontally acquired and core genome polyhydroxyalkanoate synthase genes. *PLOS ONE* **9**, e98873 (2014).
124. R. K. Bhatia, S. Ullah, M. Z. Hoque, I. Ahmad, Y. H. Yang, A. K. Bhatt, S. K. Bhatia, Psychrophiles: A source of cold-adapted enzymes for energy efficient biotechnological industrial processes. *J. Environ. Chem. Eng.* **9**, 104607 (2021).
125. J. A. Raymond, C. Fritsen, K. Shen, An ice-binding protein from an Antarctic sea ice bacterium. *FEMS Microbiol. Ecol.* **61**, 214–221 (2007).
126. H. J. Kim, J. H. Lee, Y. B. Hur, C. W. Lee, S. H. Park, B. W. Koo, Marine antifreeze proteins: Structure, function, and application to cryopreservation as a potential cryoprotectant. *Mar. Drugs* **15**, 27 (2017).
127. L. Camacho-Jiménez, A. B. Peregrino-Urriarte, J. A. Martínez-Quintana, G. Yepiz-Plascencia, The glyceraldehyde-3-phosphate dehydrogenase of the shrimp *Litopenaeus vannamei*: Molecular cloning, characterization and expression during hypoxia. *Mar. Environ. Res.* **138**, 65–75 (2018).
128. E. Willems, M. Dedobbeleer, M. Digregorio, A. Lombard, P. N. Lumapat, B. Rogister, The functional diversity of Aurora kinases: A comprehensive review. *Cell Div.* **13**, 7 (2018).
129. M. Collins, M. S. Clark, M. Truebano, The environmental cellular stress response: The intertidal as a multistressor model. *Cell Stress Chaperones* **28**, 467–475 (2023).
130. M. B. Evgen'Ev, D. G. Garbuz, O. G. Zatssepina, *Heat Shock Proteins And Whole Body Adaptation To Extreme Environments* (Springer Dordrecht, 2014).
131. G. Lopez-Martinez, M. A. Elnitsky, J. B. Benoit, R. E. Lee Jr., D. L. Denlinger, High resistance to oxidative damage in the Antarctic midge *Belgica antarctica*, and developmentally linked expression of genes encoding superoxide dismutase, catalase and heat shock proteins. *Insect Biochem. Mol. Biol.* **38**, 796–804 (2008).
132. H. J. Atkinson, P. C. Babbitt, An atlas of the thioredoxin fold class reveals the complexity of function-enabling adaptations. *PLoS Comput. Biol.* **5**, e1000541 (2009).
133. M. Rodríguez-Bolaños, H. Miranda-Astudillo, E. Pérez-Castañeda, D. González-Halphen, R. Perez-Montfort, Native aggregation is a common feature among triosephosphate isomerases of different species. *Sci. Rep.* **10**, 1338 (2020).
134. A. A. Lopez-Zavala, J. S. Carrasco-Miranda, C. D. Ramirez-Aguirre, M. López-Hidalgo, C. G. Benitez-Cardoza, A. Ochoa-Leyva, C. S. Cardona-Felix, C. Diaz-Quezada,

- E. Rudiño-Piñera, R. R. Sotelo-Mundo, L. G. Brieba, Structural insights from a novel invertebrate triosephosphate isomerase from *Litopenaeus vannamei*. *Biochim. Biophys. Acta Proteins Proteom.* **1864**, 1696–1706 (2016).
135. L. S. Peck, A cold limit to adaptation in the sea. *Trends Ecol. Evol.* **31**, 13–26 (2016).
136. S. Greco, G. Voltarel, A. S. Gaetano, C. Manfrin, A. Pallavicini, P. G. Giulianini, M. Gerdo, Comparative transcriptomic analysis reveals adaptive traits in antarctic scallop *Adamussium colbecki*. *Fishes* **8**, 276 (2023).
137. I. Raymond-Bouchard, J. Tremblay, I. Altshuler, C. W. Greer, L. G. Whyte, Comparative transcriptomics of cold growth and adaptive features of a Eury- and steno-psychrophile. *Front. Microbiol.* **9**, 1565 (2018).
138. M. R. Mangalea, B. R. Borlee, The NarX-NarL two-component system regulates biofilm formation, natural product biosynthesis, and host-associated survival in *Burkholderia pseudomallei*. *Sci. Rep.* **12**, 203 (2022).
139. B. H. Gregson, G. Metodieva, M. V. Metodiev, P. N. Golyshin, B. A. McKew, Protein expression in the obligate hydrocarbon-degrading psychrophile *Oleispira antarctica* RB-8 during alkane degradation and cold tolerance. *Environ. Microbiol.* **22**, 1870–1883 (2020).
140. Y. J. Lee, G. R. Jeschke, F. M. Roelants, J. Thorner, B. E. Turk, Reciprocal phosphorylation of yeast glycerol-3-phosphate dehydrogenases in adaptation to distinct types of stress. *Cell. Mol. Biol.* **32**, 4705–4717 (2012).
141. K. V. Ewart, R. C. Richards, W. R. Driedzic, Cloning of glycerol-3-phosphate dehydrogenase cDNAs from two fish species and effect of temperature on enzyme expression in rainbow smelt (*Osmerus mordax*). *Comp. Biochem. Physiol. B Biochem. Mol. Biol.* **128**, 401–412 (2001).
142. A. Tubeleviciute, M. G. Teese, J. Jose, *Escherichia coli* kduD encodes an oxidoreductase that converts both sugar and steroid substrates. *Appl. Microbiol. Biotechnol.* **98**, 5471–5485 (2014).
143. R. Takase, Y. Maruyama, S. Oiki, B. Mikami, K. Murata, W. Hashimoto, Structural determinants in bacterial 2-keto-3-deoxy-D-gluconate dehydrogenase KduD for dual-coenzyme specificity. *Proteins Struct. Funct.* **84**, 934–947 (2016).
144. N. Ghimire, B. Kim, C. M. Lee, T. J. Oh, Comparative genome analysis among *Variovorax* species and genome guided aromatic compound degradation analysis emphasizing 4-hydroxybenzoate degradation in *Variovorax* sp. PAMC26660. *BMC Genomics* **23**, 375 (2022).

Acknowledgments: We would like to thank A. Fumanti, E. Rastelli, and A. Sagrati for support in laboratory analyses and P. Falco for providing the environmental temperature and salinity data. **Funding:** This work was supported by the project PNRA16_00173 “Diversity and Evolution of Marine Microbial Communities associated with Antarctic Benthic Invertebrates (DEMBAI)” and by the project PNRA19_00064 “Diversity and ecological role of GIAnt Viruses in Antarctic ecosystems and consequences of ice melting on their dynamics (GIAVA).” This work was also carried out in the framework of the National Biodiversity Future Centre (Palermo, Italy). **Author contributions:** Study conception: C.C. and A.D. Sampling collection: M.L.M. Taxonomic identification of the samples: C.M. and L.M. Molecular, biochemical, and grain size analysis: E.B. Bioinformatic analysis: M.T. Phyllosymbiosis analysis: S.R. Phylogenetic analysis support: S.S. Proteomic analysis: G.P., S.T., E.E., and J.F. Writing—original draft: E.B. Writing—review and editing: C.C., M.C., A.D., M.T., and R.D. All authors participated in the final version of the manuscript. All authors have read and agreed to the published version of the manuscript. **Competing interests:** The authors declare that they have no competing interests. **Data and materials availability:** All data needed to evaluate the conclusions in the paper are present in the paper and/or the Supplementary Materials. Mitochondrial DNA sequences of the three polychaetes species have been deposited in GenBank database (<https://ncbi.nlm.nih.gov/>) with the following accession numbers: OR988154-OR988158, OR992441-OR992451, OR992452-OR992455, OR992456-OR992466, OR992467-OR992476, and OR995337. rDNA sequences of microbiomes associated with polychaetes and sediments have been deposited in GenBank database under the Bioproject PRJNA1055571 (<http://ncbi.nlm.nih.gov/bioproject/1055571>).

Submitted 19 September 2023

Accepted 14 May 2024

Published 21 June 2024

10.1126/sciadv.adk9117